UHASSELT
KNOWLEDGE IN ACTION

Maastricht University

Faculty of Medicine and Life Sciences
School for Life Sciences
Master of Biomedical Sciences

Master's thesis

Growing Better Ischemic Stroke Outcomes Using the Therapeutic Potential of Insulin-like Growth Factor-II

Emma Gesquiere

Thesis presented in fulfillment of the requirements for the degree of Master of Biomedical Sciences, specialization Molecular Mechanisms in Health and Disease

SUPERVISOR :

Prof. dr. Annelies BRONCKAERS

MENTOR :

Mevrouw Lotte ALDERS

2023
2024

Transnational University Limburg is a unique collaboration of two universities in two countries: the University of Hasselt and Maastricht University.

UHASSELT
KNOWLEDGE IN ACTION

www.uhasselt.be
Universiteit Hasselt
Campus Hasselt:
Martelarenlaan 42 | 3500 Hasselt
Campus Diepenbeek:
Agoralaan Gebouw D | 3590 Diepenbeek

UHASSELT
KNOWLEDGE IN ACTION

Maastricht University

Faculty of Medicine and Life Sciences
School for Life Sciences
Master of Biomedical Sciences

Master's thesis

Growing Better Ischemic Stroke Outcomes Using the Therapeutic Potential of Insulin-like Growth Factor-II

Emma Gesquiere

Thesis presented in fulfillment of the requirements for the degree of Master of Biomedical Sciences, specialization Molecular Mechanisms in Health and Disease

SUPERVISOR :

Prof. dr. Annelies BRONCKAERS

MENTOR :

Mevrouw Lotte ALDERS

Growing Better Ischemic Stroke Outcomes Using the Therapeutic Potential of Insulin-like Growth Factor-II*

Emma Gesquiere[1,2], Lotte Alders[2] and Annelies Bronckaers[2]
[1]Hasselt University, Campus Diepenbeek, Agoralaan building D, 3590 Diepenbeek
[2] Cardio & Organ Systems (COS) research group, Biomedical Research Institute BIOMED, Hasselt University, Campus Diepenbeek, Agoralaan building C, 3590 Diepenbeek

*Running title: *IGF-II as a therapeutic agent for ischemic stroke*

To whom correspondence should be addressed: Prof. Dr. Annelies Bronckaers, Tel: +32 (11) 26 92 23; Email: annelies.bronckaers@uhasselt.be

Keywords: Ischemic stroke, IGF-II, Neuroregeneration, Angiogenesis, Neuroprotection

ABSTRACT

Ischemic stroke is a leading cause of death and disability worldwide, yet only 15% of patients are eligible for current therapies. This underscores the need for novel treatments that meet neuroregenerative and neuroprotective demands. Insulin-like growth factor II (IGF-II) has emerged as a potential therapeutic agent due to its ability to address both strategies. This study explored the therapeutic potential of IGF-II in several key processes of neuroregeneration and neuroprotection. As IGF binding proteins (IGFBP) reduce the potency of IGF-II, a structural variant, DES[1-6]IGF-II, which is unaffected by IGFBPs, was included. Additionally, a third IGF-II variant, Leu^{27}IGF-II, which exhibits reduced binding to one of the IGF receptors, was investigated to elucidate receptor-specific actions. Our findings demonstrated increased proliferation and migration of neural stem cells (NSC) by IGF-II, evidenced by the proliferation and chemotactic transwell migration assay, respectively. Moreover, IGF-II exhibited potential angiogenic properties, as demonstrated by tube formation and CAM assays. Furthermore, by immunocytochemistry, this study demonstrated that IGF-II can potentially be neuroprotective by acting on macrophages. However, IGF-II did not reduce the infarct lesion size in a distal middle cerebral artery occlusion (dMCAO) mouse model, indicating limitations in its neuroprotective efficacy. These results suggest that IGF-II and their variants hold promise for promoting ischemic stroke-related brain repair, and future investigations are needed to further explore its therapeutic potential.

INTRODUCTION

Stroke accounts for over 1.7 million new cases and 5.5 million deaths annually, making it the second leading cause of death worldwide (1). Stroke encompasses two main pathologic types, including ischemic stroke and haemorrhagic strokes. The latter results from a blood vessel rupture, causing blood to leak into the intracranial cavity (2). In contrast, ischemic stroke stems from a sudden impaired blood flow to the brain due to a thromboembolic occlusion of a major cerebral artery. This research focuses on ischemic stroke, as this type accounts for over ~85% of all strokes globally (1, 3). The incidence rate of ischemic stroke is estimated to increase from 81.72 per 100,000 in 2020 to 89.32 per 100,000 in 2030, underscoring the importance of continued research (4).

The pathophysiology of ischemic stroke – The pathophysiology of ischemic stroke consists of numerous key processes collectively referred to as the ischemic cascade. The ischemic stroke cascade is initiated by a thromboembolic occlusion, which impairs cerebral blood flow (CBF) temporarily or permanently. The disrupted CBF deprives the brain cells of oxygen and nutrients, leading to an energetic problem within the neurons (5). Neuronal function relies on a continuous supply of adenosine triphosphate (ATP), which requires oxygen and glucose to synthesise (1). During impaired CBF, ATP consumption persists despite insufficient production (5). Upon this energy disruption, neurons lose their transmembrane gradient due to the failure of energy-dependent ion transporters (1). Subsequent influx of sodium (Na^+) and calcium (Ca^{2+}) ions and simultaneous efflux of potassium

(K^+) ions results in ionic imbalance, impaired neuronal signalling and cellular swelling (1, 5-7). The increasing Ca^{2+} concentrations trigger the depolarisation and release of the excitatory glutamate neurotransmitter (8). Glutamate, in turn, binds to the glutamate receptors, promoting another major influx of Ca^{2+} (5, 8). This pathological calcium overload sets a cascade of pathobiochemical processes into motion, resulting in neuronal degeneration (9). It involves the activation of proteases and nucleases, leading to the breakdown of the cell membrane and the DNA. This extensive cell damage initiates apoptosis, necrosis and autophagy-mediated cell death (1, 5, 7). The excessive Ca^{2+} levels also impair mitochondrial functions, triggering the production of reactive oxygen species (ROS), such as nitric oxide (NO), superoxide (O_2^-) and hydroxyl ($OH\cdot$) radicals (10). The generated ROS harms mitochondrial components, promoting the release of apoptotic signals and subsequent apoptosis. The region of permanent brain damage forms the infarct core region (1). This region is surrounded by the penumbra, where collateral pathways may form. Collaterals maintain CBF and prevent total CBF arrest. Despite falling below the functional threshold, CBF levels remain above the threshold for cell death (5). This implies compromised cellular function while cell viability persists for a limited time period in the penumbra (1, 5). Timely reperfusion can save these cells. However, failure to achieve on-time reperfusion leads to core region expansion, resulting in more permanent damage. This, in turn, leaves patients with a poor quality of life, as this damage can lead to physical and cognitive impairments, such as paralysis, sensory disturbances, and aphasia (11).

The blood-brain barrier (BBB) is an indispensable physicochemical barrier separating the central nervous system (CNS) from the systemic circulation, sustaining CNS homeostasis and protecting brain tissue (12). After ischemic stroke, the permeability of the BBB increases due to the breakdown of the endothelial basal lamina by proteases released from damaged neurons, glial cells and endothelial cells (6). The increased permeability and barrier integrity disruption allows for the penetration of peripheral immune cells, including neutrophils, macrophages, natural killer cells, dendritic cells, T cells and B cells, into the ischemic lesion (13). The migration of these peripheral immune cells and the activation of brain resident cells, such as microglia, contribute to the brain's neuroinflammation. Over the course of days to weeks, a complex influx of inflammatory cells takes place (5). Within the first hours after the stroke onset, neutrophils are the first immune cells to infiltrate the ischemic lesion and can last up to 15 days post-injury (13, 14). Neutrophils induce secondary injury by releasing ROS, proteases, pro-inflammatory factors and matrix metalloproteinases, causing further BBB disruption and post-ischemia oedema (14). Next, T lymphocytes invade the lesion within the first 24 hours and can last up to 30 days (13, 15). T cells promote the adhesion of platelets and leukocytes to the vascular endothelium, causing thrombo-inflammation, exacerbating neuroinflammation (15). Lastly, monocytes and macrophages arrive at the ischemic lesion, portraying a dual role by both aggravating and mitigating the ischemic lesion. During the acute phase after stroke, macrophages display a pro-inflammatory state, exacerbating ischemic stroke progression via enhancing neuroinflammation. As the stroke advances, these macrophages transition to a pro-regenerative and protective state, resulting in the clearance of cellular debris via phagocytosis and the secretion of trophic factors, promoting brain repair (13). Similar to macrophages, the brain resident microglia are initially considered to be neurotoxic while also shifting towards a pro-reparative state (5, 6).

Despite the extensive research on stroke over the last decades, no simple means of treating ischemic stroke has been established (3). Current therapies focus on restoring the CBF to salvage the penumbra and prevent further brain tissue damage. Currently, approved interventions for ischemic stroke are limited to thrombolysis and thrombectomy. Thrombolysis is the dissolution of the thrombus using tissue Plasminogen Activator (tPA) (16). tPA has proven to be effective when administered within 4.5 hours of stroke onset. However, the use of tPA is associated with inherent risks; tPA can result in haemorrhage, which can be, in some cases, life-threatening (16). Thrombectomy is the surgical removal of the thrombus (16). This method provides a time window of up to 8 hours after onset (16, 17). Despite the effectiveness of both therapies, they result in only 15% of patient eligibility due to the relatively short time window (1). Additionally, these therapies solely aim to

prevent further brain damage. These restraints highlight the need for novel therapeutic interventions to increase patient eligibility and provide long-term therapeutic potential. Promising strategies include targeting neuroprotection and neuroregeneration.

Neuroprotective strategies in ischemic stroke – Neuroprotection is defined as an effect that results in the preservation and recovery of the CNS, its cells, structure, and function by inhibiting the pathogenic stroke cascade (18). A crucial aspect in the progression of ischemic stroke is the infiltration of macrophages; in the acute phase of ischemic stroke, they present a more pro-inflammatory and disease-stimulating state (13). Nevertheless, these macrophages can switch to a more pro-regenerative state in later stages, which can benefit stroke repair (13). Considering the dual role of macrophages, they became interesting therapeutic targets for neuroprotective strategies as their anti-inflammatory and disease-resolving state can be used to undermine neuroinflammation.

Neuroregenerative strategies in ischemic stroke – The ability of the ischemia-damaged CNS to self-repair is minimal, so finding ways to stimulate this regenerative capacity will revolutionise stroke therapy (19). Neurogenesis, which is the formation of new neurons from neural stem cells (NSC), occurs in two primary regions of the brain: the subventricular zone (SVZ) of the lateral ventricles and the subgranular zone (SGZ) of the dentate gyrus in the hippocampus (11). In order to give rise to new functional neurons during stroke recovery, NSC must proliferate, migrate towards the lesion, differentiate into functional neurons, and collectively integrate into the local circuitry of the brain (11). Regulating neurogenesis post-stroke is a delicate process in which the environment is an essential factor. Several studies have discovered that a stroke-induced environment stimulates neurogenesis and induces neuroregenerative repair (20-22). However, other studies have reported that newborn neuron survival is strongly reduced due to the post-stroke micro-environment lacking neurotrophic factors and chronic inflammatory responses (23). These findings open a novel therapeutic opportunity to target and stimulate neurogenesis by establishing a post-stroke environment that stimulates neurogenesis.

As newly formed neurons require nutrients and oxygen to become functional and survive in the infarcted region, the formation of new blood vessels, also known as angiogenesis, emerges as another crucial aspect of neuroregeneration. Angiogenesis is closely intertwined with neurogenesis after stroke, as both processes seem to stimulate each other (23). New blood vessels arise via the sprouting of preexisting vessels, and it encompasses key phases, including the proliferation and migration of endothelial cells, followed by the formation of tube-like structures forming the complete blood vessel (23). Both preclinical and clinical studies have shown that following ischemic stroke, angiogenesis occurs in the peri-infarct regions and that it positively correlates with survival and recovery (24-27).

Compelling evidence underscores the importance of neurogenesis, angiogenesis and a reparative-friendly environment via the modulation of neuroinflammation in facilitating ischemic stroke repair. This points towards a novel therapeutic avenue for exploring compounds that can effectively stimulate these three crucial aspects.

Insulin-like growth factors (IGF) – The IGF-axis is a hormonal network regulating cell growth, proliferation and survival. It affects nearly every organ system, including the CNS (28). This axis includes three ligands, called insulin, IGF-I and IGF-II, their receptors and IGF binding proteins (IGFBPs) (29). IGF-I and IGF-II are anabolic, single-chain polypeptides (70 and 67 amino acids, respectively), sharing homology with each other and proinsulin (30). Whereas these three insulin-like peptides are expressed in the developing brain, evidence indicates that IGF-II expression is the highest in the adult brain, primarily produced by the choroid plexus, leptomeninges and endothelial cells (31, 32). The actions of IGF-II are mediated through three different receptors encompassing the insulin receptor (IR), IGF receptor type 1 (IGFR1) and type 2 (IGFR2). The former two are tyrosine kinase receptors leading to activation of the downstream Ras-mitogen-activated protein kinase (MAPK) and phosphoinositide 3 kinase (PI3K) signalling pathways upon ligand binding (33-35). Activation of these pathways ultimately leads to downstream cellular proliferation, migration, survival and differentiation functions via other intracellular molecules (30, 35). The IGFR2 is

identical to a cation-independent mannose-6-phosphate (M6P) receptor, which IGF-II can activate exclusively. This receptor is a single-chain transmembrane protein mainly responsible for controlling circulating IGF-II levels by targeting IGF-II for internalisation and lysosomal degradation (32, 35). However, several studies have postulated the involvement of IGFR2 in angiogenesis, as demonstrated by *in vitro* angiogenesis assays (36, 37). An important component of the IGF-axis is the presence of IGFBPs in biological fluids (i.e. blood and cerebrospinal fluid). Currently, six high-affinity IGFBPs (IGFBP1-6) and four low-affinity IGFBPs have been identified (30, 35). These six highly conserved IGFBPs share the same structure with two subdomains: highly conserved cysteine-rich N- and C-terminals contributing to the high-affinity IGF binding (35). IGFs, but not insulin, are non-covalently bound to high-affinity IGFBP-1 to -6 in all biological fluids, in which they modulate their action (38). Of all IGFBPs, IGFBP-6 has the highest affinity for IGF-II compared to the other IGFBPs and is widely expressed in the brain (39). IGFBPs bind IGF-I and IGF-II with higher affinity than the cell surface receptors, limiting the bioavailability of IGFs for receptor activation (35). To overcome this limitation, an innovative structural variant called DES[1-6]IGF-II was included in this research. DES[1-6]IGF-II lacks the first six amino acids from the N-terminus, which is responsible for binding to IGFBPs, suggesting that it may have increased potency (40). DES[1-6]IGF-II still display similar affinities for the IGF receptors compared to wild-type IGF-II (41). Although reducing the availability of IGF-II is considered detrimental, IGFBPs also play important functions in physiological processes. IGFBPs extend the half-life of IGFs from 10 minutes to approximately 30-90 minutes (35, 42). IGFs also lack tissue stores; therefore, IGFBPs facilitate the accumulation of large reservoirs of IGFs within the body (35). Finally, IGFBPs also function as transport proteins in plasma and determine the tissue and cell-specific localisation of IGFs (30). This study also includes a third IGF-II variant, namely Leu^{27}IGF-II. Leu^{27}IGF-II has a Leucine substitution in place of Tyrosine at position 27 of the IGF-II sequence. This substitution results in a 10-20-fold reduction in binding to the IGFR1 compared to IGFR2. This variant can provide insights into which receptors are involved in the neuroregenerative or neuroprotective effects of IGF-II.

Recent studies described the neuroprotective properties of IGF-II regarding neuroinflammation. A study on inflammation-induced mice described that IGF-II administration prevents a pro-inflammatory state switch of microglia, thereby reducing overall neuroinflammation (43). Additionally, a study on maturing macrophages reported that IGF-II preprogrammes maturing macrophages to acquire anti-inflammatory properties (44). Also, neuroregenerative properties of IGF-II have been described. Bracko *et al.* demonstrated that IGF-II controls NSC proliferation *in vitro* and *in vivo* (45). In general, several studies found that IGF-II promotes neurogenesis in the SVZ and the SGZ of the adult brain (45-47). Substantial evidence also shows a possible contribution of IGF-II to angiogenesis. Knockdown of IGF-II and IGFR1 inhibited angiogenesis in developing mouse retina and in zebrafish (48, 49). Additionally, IGF-II induced by hypoxia also stimulated angiogenesis in human hepatocellular carcinoma (50).

The potential therapeutic efficacy of IGF-II in ischemic stroke emerges from its purported neuroprotective and neuroregenerative properties. Nevertheless, the intricate cellular processes through which IGF-II may facilitate neuroprotection by attenuating neuroinflammation and promoting neuroregeneration, including neurogenesis and angiogenesis, remain elusive. Furthermore, to date, no extensive research has been conducted on DES[1-6]IGF-II in the context of neuroprotection and neuroregeneration.

In addressing these research gaps, the present study explores IGF-II, DES[1-6]IGF-II and Leu^{27}IGF-II as potential therapeutic agents in the context of neuroprotection and neuroregeneration after ischemic stroke. It is hypothesised that all IGFs stimulate neuroregeneration by promoting neurogenesis and angiogenesis and that they have the potential to be neuroprotective by acting on macrophages. In addition, it is hypothesised that when IGFBP-6 is present, the effects of IGF-II are reduced while the effects of DES[1-6]IGF-II remain.

EXPERIMENTAL PROCEDURES

Cell culture – All cell experiments and all cells were cultured at 37°C in a 5% CO_2 atmosphere

incubator. Culture media and supplements used for the different cell types can be found in Table S1. Neural stem cells (NSC) were isolated and cultured according to Gervois *et al. (51)*. When cells reached 80% confluency, they were subcultured using accutase for detachment. For cell culture and experiments involving NSC, all culture material was coated with 5 µg/ mL Fibronectin (1030-FN-05M, R&D Systems, USA). Human microvascular endothelial cells (HMEC-1) were kindly provided by the Centers for Disease Control and Prevention (Atlanta, GA, USA). 0.05% Trypsin/EDTA (T3924, Sigma, Germany) was used to detach cells for subculturing when cells reached a confluence of 80%. The Raw264.7 cells were kindly provided by Dr. Paula Pincela Lins. When the cells reached 70% confluence, they were detached by scraping and subcultured. Bone marrow-derived macrophages (BMDM) were kindly provided by Dr. Jana Van Broeckhoven.

Immunocytochemistry (ICC) – NSC (passage 26), HMEC-1 (passage 8), Raw264.7 (passage 7), and BMDM cells were seeded at a density of 50,000, 25,000, 20,000, and 150,000 cells per well in a 24-well plate, respectively. After attachment, cells were fixed with 4% paraformaldehyde (PFA) for 15 minutes at room temperature (RT). Prior to fixation, Raw264.7 cells were stimulated with 100 ng/mL LPS (L2637-5MG, Merck, Germany**)** and 10 ng/mL IFN-γ (300-02, Peprotech, Belgium) for 24 hours or left unstimulated. BMDMs were stimulated with 200 ng/mL LPS (L2637-5MG, Merck) for 12 hours of left unstimulated. The cells were blocked with 100% protein block (PB) (X0909, Dako, USA) for 20 minutes at RT to prevent aspecific binding. Primary antibodies (Table S3) were diluted in 10% PB and incubated overnight at 4°C. Next, the secondary antibodies (Table S3) and Hoechst (1/5000) (Molecular probes, H-3570, The Netherlands) were diluted in 10% PB and incubated for 1 hour at RT in the dark. Slides were mounted with anti-fade Immu-mount (9990402, Thermofisher Scientific, USA), and images were captured using the LeicaDM2000 LED fluorescence microscope and Leica Application Suite X software (Leica Microsystems).

Cell proliferation assay – To evaluate the effect of IGF-II on NSC proliferation, a proliferation assay was used. 5,000 NSC cells (passage 21-26) were seeded in standard culture medium (Table S1). Twenty-four hours later, they were treated with different test conditions (Table S2). Images were captured every two hours using the IncuCyte® S3 Live-Cell Analysis System (Sartorius, Germany) for five days. The acquired confluence was normalised against the confluence at timepoint 0 h. The assay was performed three times with 2-4 technical replicates per condition.

Transwell migration assay – The chemotactic capacity of IGF-II on NSC was evaluated using the transwell migration assay. 5,000 NSC cells (passage 19-24) were seeded in transwell medium (Table S2) in the insert of an Incucyte® Clearview 96-well chemotaxis plate (4648, Sartorius, 8µm). After 30 minutes of settling, test conditions (Table S2) were added to the bottom compartment. The inserts were placed on the bottom compartment and incubated for five days. Every two hours, an image was taken and analysed using the chemotaxis tool of the IncuCyte® S3 Live-Cell Analysis System (Sartorius). Migration was quantified as the cell surface area of migrated cells (bottom) normalised to the surface area occupied by the non-migrated cells (top) at timepoint 4 h. The assay was performed five times, including 3-4 technical replicates per condition.

Tube formation assay –To examine the effect of IGF-II on endothelial tubulogenesis, a tube formation assay was performed. Wells of a 96-well plate were coated with GF-reduced Matrigel (354230, Corning, USA) basement membrane and incubated for 60 minutes to allow setting. After polymerisation, a suspension containing test conditions (Table S2) and 20,000 HMEC-1 cells (passage 7-11) were **s**eeded. Tube formation was monitored using the IncuCyte® S3 Live-Cell Analysis System (Sartorius). Images were captured after 6 hours and were analysed using ImageJ Software with the Angiogenesis analyser plug-in (52). This assay was performed three times, including 2-3 technical replicates.

ELISA – To evaluate the concentration of several secreted angiogenic factors, ELISA's were performed. The concentration of IL-6 (430504, BioLegend, USA), uPAR (448404, BioLegend) and MCP-1 (438804, Biolegend) was measured in the conditioned medium from HMEC-1 cells (passage 6-10) treated with different test conditions for 48 hours (Table S2). ELISAs were performed according to the manufacturer's instructions. The absorbance was measured with the CLARIOstar

Plus (BMG Labtech, Germany) plate reader. A standard curve was set up to determine the concentration of the secreted factors. This assay was performed 1-2 times with nine biological replicates.

Chorioallantoic membrane (CAM) assay – A CAM assay was performed to determine the angiogenic potential of IGF-II *in ovo*. Fertilised chicken eggs (Gallus Gallus) were incubated at 37°C and 50% humidity. On embryonic day 3 (E3), 3-4 mL of albumin was removed to detach the CAM from the eggshell and the eggs were returned to the incubator. At E9, absorbent gelatin sponges (ZHG805001, SMI AG, Belgium) with test conditions were placed onto the CAM (Table S2). At E12, the CAM was removed and photographed with a digital camera (HandyCam HDR-XR350VE, Sony, UK). Angiogenesis was assessed by counting blood vessels intersecting two digitally placed concentric circles with a radius of 1 and 2 mm. Counting was performed blindly by three independent investigators.

Permanent distal middle cerebral artery occlusion (dMCAO) – 10-week-old male C57BL/6 mice (Envigo, Horst, The Netherlands) were subjected to permanent dMCAO as previously described (53). Animals were housed under standardised conditions (12h light-dark cycle and a temperature of 20°C ± 3°C). Food and water were provided ad libitum. Experiments were approved by the Ethical Committee for Animal Experimentation of Hasselt University.

Immunofluorescent (IF) staining of healthy and dMCAO brain coupes – IF stainings were performed on brain tissues from healthy and dMCAO mice. The brains were isolated three and seven days post-stroke and fixed in 4% PFA for 24 hours. Next, brain tissues were embedded in paraffin and sliced into 7 µm thick coupes. They were baked at 58°C for one hour prior to undergoing xylene deparaffinisation, followed by ethanol gradient (100%-75%) hydration and distilled H_2O hydration. Antigen retrieval was performed for 30 minutes in a 95°C warm water bath using citrate buffer (10 mM Sodium citrate, 0.05% Tween20, pH 6.0). After PBST (1x PBS 0.1% Triton X-100) wash, the brain coupes were blocked with 100% PB (X0909, Dako) for one hour to prevent aspecific binding. After blocking, the brain coupes were incubated with primary antibodies (Table S4) diluted in 10 % PB overnight at 4°C. Next, the brain coupes were incubated with the secondary antibodies (Table S4) and Hoechst (1/5000, Molecular probes, H-3570) diluted in 10 % PB for one hour in the dark. Finally, sections were mounted with Immu-mount (Thermo Scientific – 9990402), and images were captured using the LeicaDM2000 LED fluorescence microscope and Leica Application Suite X (LAS X) software (Leica Microsystems). Images were processed with ImageJ software.

IGF-II treatment - One hour after dMCAO, mice were randomised and treated with vehicle control (HCl 10mM), IGF-II (FU100, Gropep, Australia) or DES[1-6]IGF-II (MU100, Gropep) at 0.02, 0.1 or 0.5 µg via stereotactical injection. Twenty-four hours after injection, mice were sacrificed via cervical dislocation and the brains were isolated for 2.3.5-Triphenyltetrazolium chloride (TTC*)* staining.

2.3.5-Triphenyltetrazolium chloride (TTC) staining – To determine the infarct lesion volume, a TTC staining was performed on isolated brains. 1mm coronal slices were cut using steel blades (Ted Pella, USA) and Alto steel brain matrix (Stoelting, Ireland). The slices were stained for 30 minutes at RT using a 2% TTC solution (17779, Sigma-Aldrich). The stained brain coupes were scanned with a printer, and the infarct volume was quantified blindly using ImageJ software. The percentage of total stroke lesion area was calculated.

Statistical analysis – Statistical analysis was performed using GraphPad Prism 10 software (GraphPad, La Jolla, USA). Normality was checked using the Shapiro-Wilk test. In case normality was fulfilled, three or more experimental groups were compared using an RM or ordinal one-way ANOVA with Dunnett's or Sídák's post hoc test. In case normality was not fulfilled, a nonparametric Friedmann test with Dunn's post hoc test was used. To compare two groups, a paired t-test, an unpaired t-test or, in case normality was not fulfilled, the Mann-Whitney test was used.

RESULTS

IGF-II enhances neurogenesis by stimulating NSC proliferation in vitro – Neuroregeneration is essential for complete brain repair following ischemic stroke and can be divided into neurogenesis and angiogenesis. Given the crucial role of neurogenesis in stroke recovery, this study

first examined the influence of IGF-II on this process. The initial stage of neurogenesis involves the proliferation of NSC. Before testing the effect of IGF-II on the growth of NSC, it was necessary to determine the susceptibility of NSC to IGF-II. Via immunocytochemistry, the presence of all three IGF-II receptors—IGFR1, IGFR2, and IR— was confirmed (Fig. 1A). Next, the effect of IGF-II on NSC proliferation *in vitro* was examined by assessing the confluence over time (Fig. 1C). Compared to the HCl control, IGF-II significantly increased NSC proliferation by 38.6% at 72 hours, as indicated by the enhanced cell confluency (Figures 1B and 1E). Similarly, DES[1-6]IGF-II also promoted cell confluence, thereby significantly stimulating NSC proliferation by 16% at 48 hours and showing a trend towards increased proliferation of 26% at 72 hours compared to the HCl control (Figures 1D and 1E). Leu^{27}IGF-II, however, does not alter the proliferation of NSC at 48 hours or 72 hours compared to the HCl controls (Figures 1D and 1E).

IGF-II stimulates neurogenesis by enhancing chemotactic NSC migration in vitro – Following proliferation, NSC migration towards the infarcted area is the next crucial step in neurogenesis. Two distinct migration assays were conducted to evaluate the potential of IGF-II in stimulating NSC migration. A scratch-wound healing assay was performed to assess the direct effect of IGF-II on NSC migration. This assay, containing IGF-II concentrations ranging from 0.001 ng/mL up to 1000 ng/mL, revealed that IGF-II did not directly stimulate NSC migration (Fig. S1). Next, a transwell migration assay was performed to investigate the chemotactic properties of IGF-II. Compared to the HCl control, NSC indeed responded to the chemotactic signals of IGF-II and DES[1-6]IGF-II at a concentration of 100 and 1000 ng/mL at 72 hours (Fig. 2A-D). IGF-II at 100 and 1000 ng/mL increased NSC migration by 156% and 334%, respectively (Figures 2B and 2D). Moreover, DES[1-6]IGF-II at 100 and 1000 ng/mL increased NSC migration by 147% and 300%, respectively (Figures 2B and 2D). Leu^{27} IGF-II again did not elicit any response of chemotactic NSC migration at 100 (48.8%) and 1000 ng/mL (22.8%) (Fig. 2A-D.). We extended our investigation to explore the impact of IGFBP-6 on the chemotactic effects of IGF-II. Although the presence of IGFBP-6 showed no significant effect, a notable downward trend of 49.9% and 13% was observed for 100 and 1000 ng/mL IGF-II, respectively (Figures 2E and 2F). Remarkably, IGFBP-6 markedly reduced the effectiveness of DES[1-6]IGF-II by 20.3% and 31.9% at both 100 and 1000 ng/mL (Figures 2E and 2F).

IGF-II has the potential to stimulate angiogenesis in vitro – Beyond neurogenesis, the other critical component of neuroregeneration is angiogenesis, the formation of new blood vessels. This process is essential for vascularising newly formed brain tissue to supply oxygen and nutrients. Therefore, this research investigated the angiogenic potential of IGF-II *in vitro*. Initially, the presence of all three IGF-II receptors on HMEC-1 cells was visualised via immunocytochemistry (Fig. 3A). Previous work from our research group identified several angiogenic factors upregulated in HMEC-1 endothelial cells by IGF-II using a cytokine array (data not shown). Consequently, these results were validated by measuring the concentrations of these secreted angiogenic factors, including, interleukin 6 (IL-6), monocyte chemoattractant protein-1 (MCP-1) an urokinase plasminogen activator surface receptor (uPAR), via ELISA. The results showed that conditioned media from IGF-II-treated and DES[1-6]IGF-II-treated HMEC-1 cells exhibited increased expression of all three angiogenic factors compared to the their control medium (Fig. 3B-D). IL-6 displayed the most substantial increase in expression by IGF-II (13.02 ± 4.62 vs 3.25 ± 1.97) and DES[1-6]IGF-II (12.91 ± 3.87 vs 3.25 ± 1.97), compared to the their control medium (Fig. 3B). MCP-1 expression was also strongly increased by IGF-II (32.62 ± 12.48 vs 17.40 ± 6.81) and DES[1-6]IGF-II (33.52 ± 12.1 vs 17.40 ± 6.81) compared to their control medium (Fig. 3C). Finally, uPAR showed a modest increased expression by IGF-II (156.3 ± 81.4 vs 136.9 ± 79.86) and DES[1-6]IGF-II (158.4 ± 82.04 vs 136.9 ± 79.86) compared to their control medium (Fig. 3D). Addition of IGFBP-6 significantly reduced the stimulatory effect of IGF-II on all three angiogenic factors with 59.2% (IL-6), 47.5% (MCP-1), and 13.6% (uPAR). (Fig. 3B-D). While IGFBP-6 also significantly diminished the effect of DES[1-6]IGF-II on IL-6 secretion by 20.4%, this reduction was less pronounced than IGF-II (Fig. 3B). For MCP-1 and

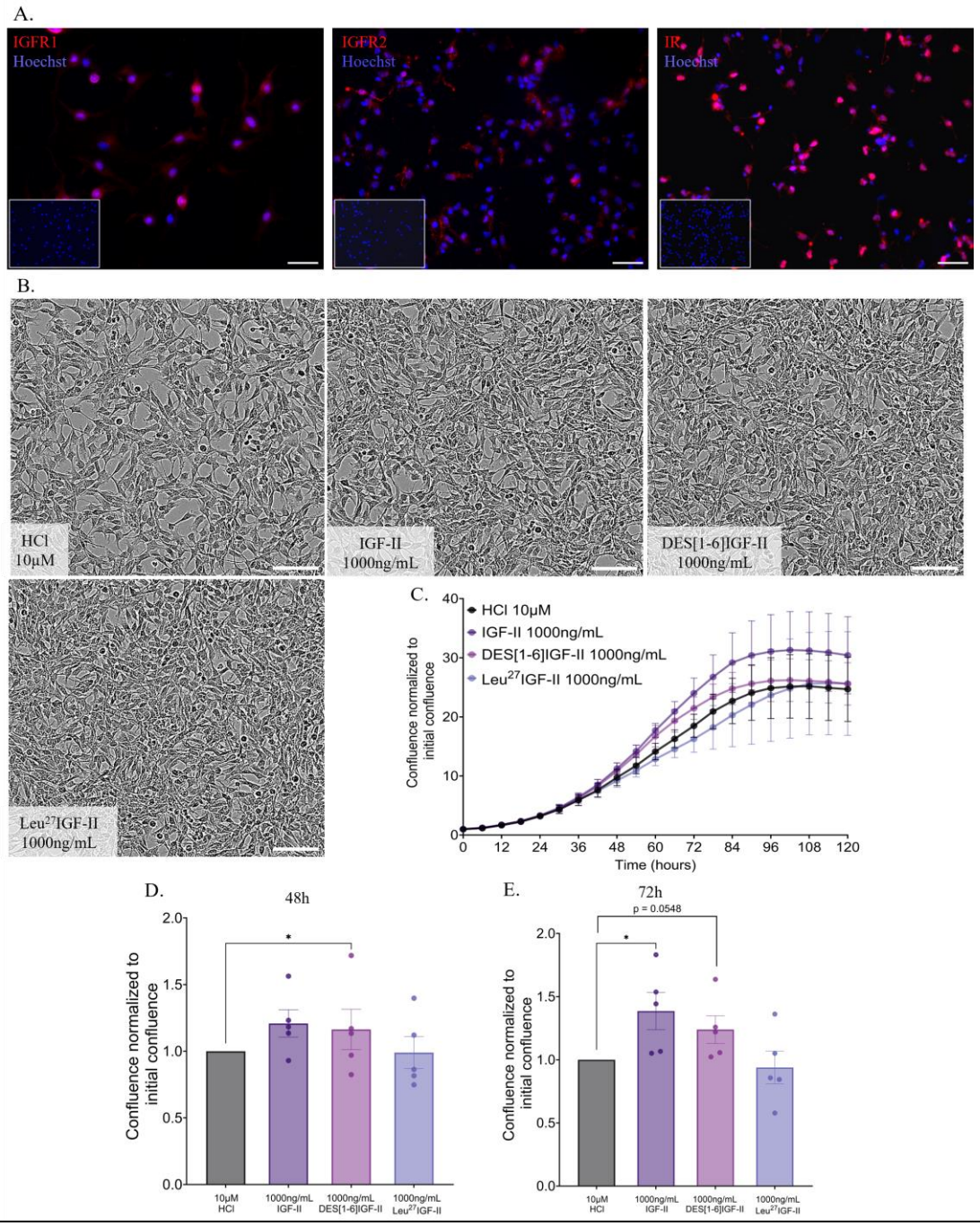

Figure 1 – **IGF-II Stimulates Neural Stem Cell Proliferation. A.** Representative images of immunocytochemistry staining show the presence of the three IGF-II receptors – IGFR1 (left panel), IGFR2 (middle panel), and IR (right panel) - on NSC. Nuclei were counterstained with Hoechst (blue). Insert shows the negative control. Scale bar represents 30µm. **B.** Representative images of the proliferation assay displaying cell confluence for the HCl control, IGF-II, DES[1-6]IGF-II and Leu^{27}IGF-II at 72 hours. Scale bar represents 200µm. **C.** The effects of IGF-II, DES[1-6]IGF-II and Leu27IGF-II on the proliferation of NSC over a period of five days are shown. The graph presents the mean confluence area normalised to the initial confluence at timepoint 0h. **D.** After 48 hours, 1000 ng/mL DES[1-6]IGF-II significantly stimulates NSC proliferation. **E**. After 72 hours, IGF-II at 1000 ng/mL significantly stimulates NSC proliferation, while DES[1-6]IGF-II shows a strong trend towards stimulating NSC proliferation. **C-E.** Data are expressed as mean ± SEM. N = 5 with 2-4 replicates per condition. Each data point represents an independent assay. *p<0,05. Statistical analysis was performed using the RM one-way ANOVA with Dunnett's post hoc test. *HCl, hydrochloric acid; IGF, insulin-like growth factor; IGFR1, insulin-like growth factor receptor type 1; IGFR2, insulin-like growth factor receptor type 2; IR, insulin receptor; NSC, neural stem cells; RM, repeated measures; SEM, standard error of the mean.*

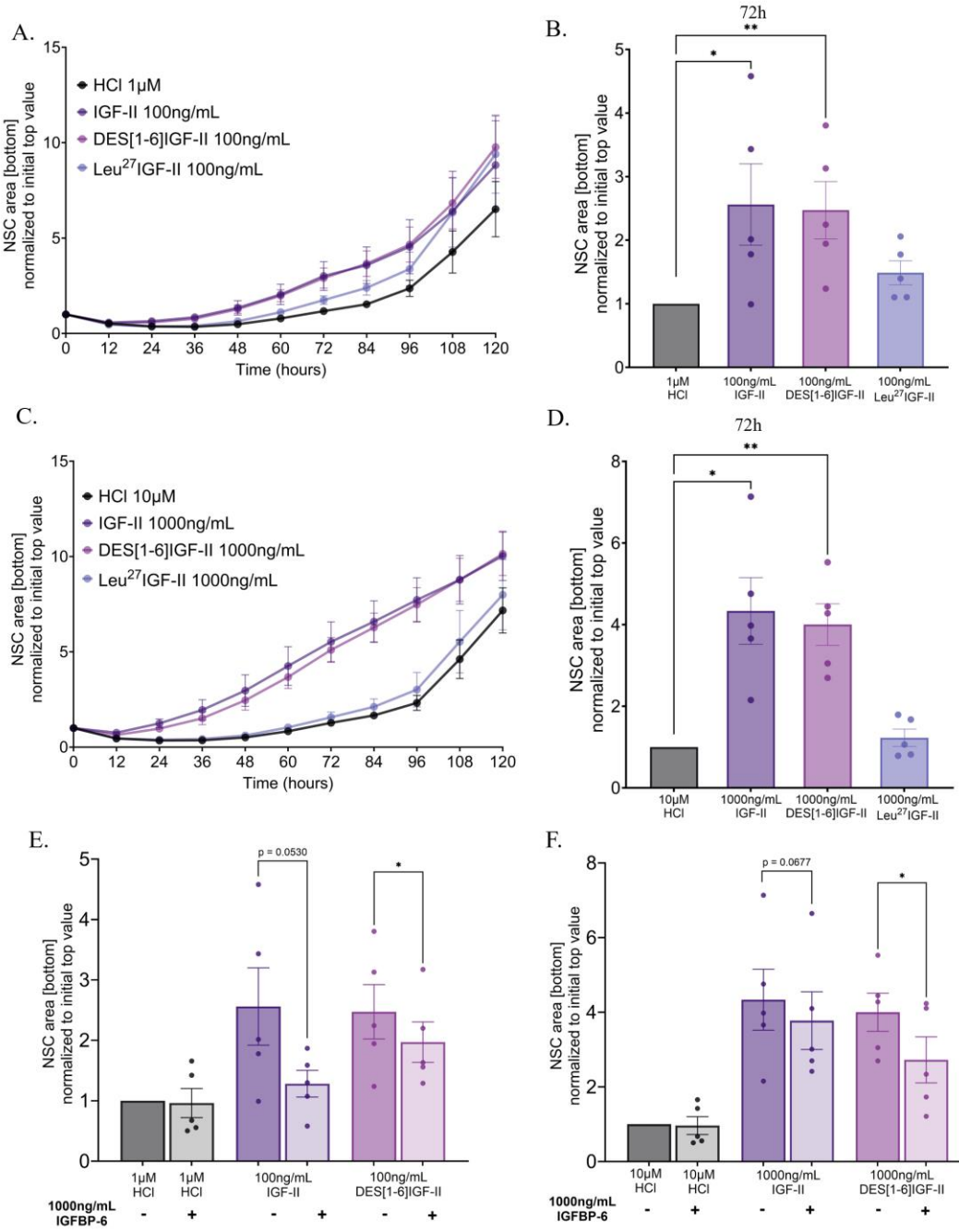

Figure 2 – **IGF-II Stimulates Neural Stem Cell Migration via Chemotaxis.** The effects of IGF-II, DES[1-6]IGF-II and Leu27IGF-II on NSC migration were assessed using a transwell migration assay. **A and C.** The graphs illustrate the mean NSC area in the bottom compartment normalised to the initial top area and relative to their HCl control for the three IGF variants over five days. After 72 hours, IGF-II and DES[1-6]IGF-II at concentrations of **B.** 100 ng/mL and **D.** 1000 ng/mL significantly stimulated the migration of NSC. **E-F.** The impact of IGF binding protein 6 (IGFBP-6) on the ability of IGF-II and DES[1-6]IGF-II to stimulate NSC migration was also examined. IGFBP-6 at 1000 ng/mL trendily decreased the effect of **E.** 100 ng/mL IGF-II and **F.** 1000 ng/mL IGF-II and significantly reduced the effects of DES[1-6]IGF-II. **A-F** Data are expressed as mean ± SEM. N = 5 with 4 replicates per condition. Each data point represents an independent assay. *p<0.05; **p<0.01. Statistical analysis was performed using RM one-way ANOVA with Dunnett's and Sídák's post hoc test or the non-parametric Friedmann test with Dunn's post hoc test for comparing three or more groups. A paired t-test was used to compare the two groups. *HCl, hydrochloric acid; IGF, insulin-like growth factor; IGFBP-6, IGF binding protein 6; NSC, neural stem cells; RM, repeated measures; SEM, standard error of the mean.*

uPAR, IGFBP-6 did not appear to significantly impact the effect of DES[1-6]IGF-II (Figures 3C and 3D).

The angiogenic potential of IGF-II was further investigated by assessing its role in the tubulogenesis of HMEC-1 cells using a tube formation assay. This assay evaluated key angiogenesis parameters, including total segment length (Fig. 3E – magenta) and total branch length (Fig. 3E – green). HMEC-1 cells treated with 100 ng/mL or 1000 ng/mL IGF-II, DES[1-6]IGF-II, or Leu27IGF-II did not exhibit significantly more segments or branches compared to the HCl control (Figures 3F, 3G, S2A and S2B). However, a visual examination of total segments indicated a positive trend in all three IGF variants (Fig. 3E).

IGF-II demonstrates a tendency to stimulate angiogenesis in ovo – The potential of IGF-II to induce angiogenesis was assessed using the chick chorioallantoic membrane (CAM) assay. At E3, 3mL albumin was removed, and a treatment window was made by removing a small part of the eggshell. At E9, absorbent-gelatin sponges were placed onto the CAM, followed by isolation of the CAM three days later (Fig. 4A). Compared to the HCl control, IGF-II at concentrations of 0.5 ng ($p = 0.0857$) and 50 ng ($p = 0.0680$) strongly tend to stimulate angiogenesis within a two-millimetre radius (Fig. 4B-D). However, beyond this range at 4 mm, IGF-II did not stimulate angiogenesis at either concentration compared to HCl (Fig. 4B-D).

IGF-II has the potential to be neuroprotective by acting on macrophages – This study investigated whether IGF-II could potentially exert neuroprotective effects by demonstrating the expression of the three IGF-II receptors on macrophage cell lines and bone marrow-derived macrophages (BMDM) (Fig. 5A-D). Specifically, this study showed that both resting macrophages (M0) and pro-inflammatory macrophages (LPS and IFN-y stimulated) of both cell types express all three IGF-II receptors (Fig. 5A-D). Furthermore, this study also demonstrated the presence of ionised calcium-binding adapter molecule 1 (Iba1) in and near the infarct lesion of a distal middle cerebral artery occlusion (dMCAO) mouse brain one week after stroke onset (Fig. 5E). Iba-1 is a well-known marker to highlight the presence of macrophages and microglia.

All three IGF-II receptors are present in healthy or stroke brain tissue – This study also identified the presence of the three IGF-II receptors in healthy murine brain tissue as well as in brain tissue from dMCAO mice three and seven days post-stroke (Fig. S3-S5). Here, it was found that IR and IGFR1 were present in healthy brain tissue, while IGFR2 seemed to be absent (Fig. S3). At three days post-stroke, IGFR2 seemed to be strongly present, while IGFR1 and IR displayed barely any presence (Fig. S4). Finally, at seven days post-stroke, the IR and, to a lesser extent, IGFR1 were present, while the IGFR2 seemed absent (Fig. S5). Furthermore, several IF markers were tested to identify a marker that visualised the stroke region clearly. This study identified neurofilament 68kD (NF) as the best marker to visualise the lesion area (Figure S6).

IGF-II does not reduce the infarct lesion size in a dMCAO mouse model –To investigate whether IGF-II harbours neuroprotective properties, meaning reducing stroke infarct size mice were subjected to stroke. The dMCAO model was achieved via electrocoagulation proximal and distal to the bifurcation of the middle cerebral artery (MCA). One hour after dMCAO induction, mice received intracerebroventricular injections of IGF-II and DES[1-6]IGF-II through stereotactic injections. After 24 hours, the mice were sacrificed by cervical dislocation, and their isolated brains were stained with TTC dye to visualise the stroke lesion (Fig. 6A). Neither IGF-II nor DES[1-6]IGF-II at any concentration reduced the infarct lesion size compared to the vehicle control (Figures 6B and 6C). It seems that only IGF-II at 0.5 µg (2.96 ± 2.24 vs 4.51 ± 4.06) showed a decreased trend in lesion size compared to vehicle control, while all other test conditions visually showed a slightly increased lesion size (Fig. 6C).

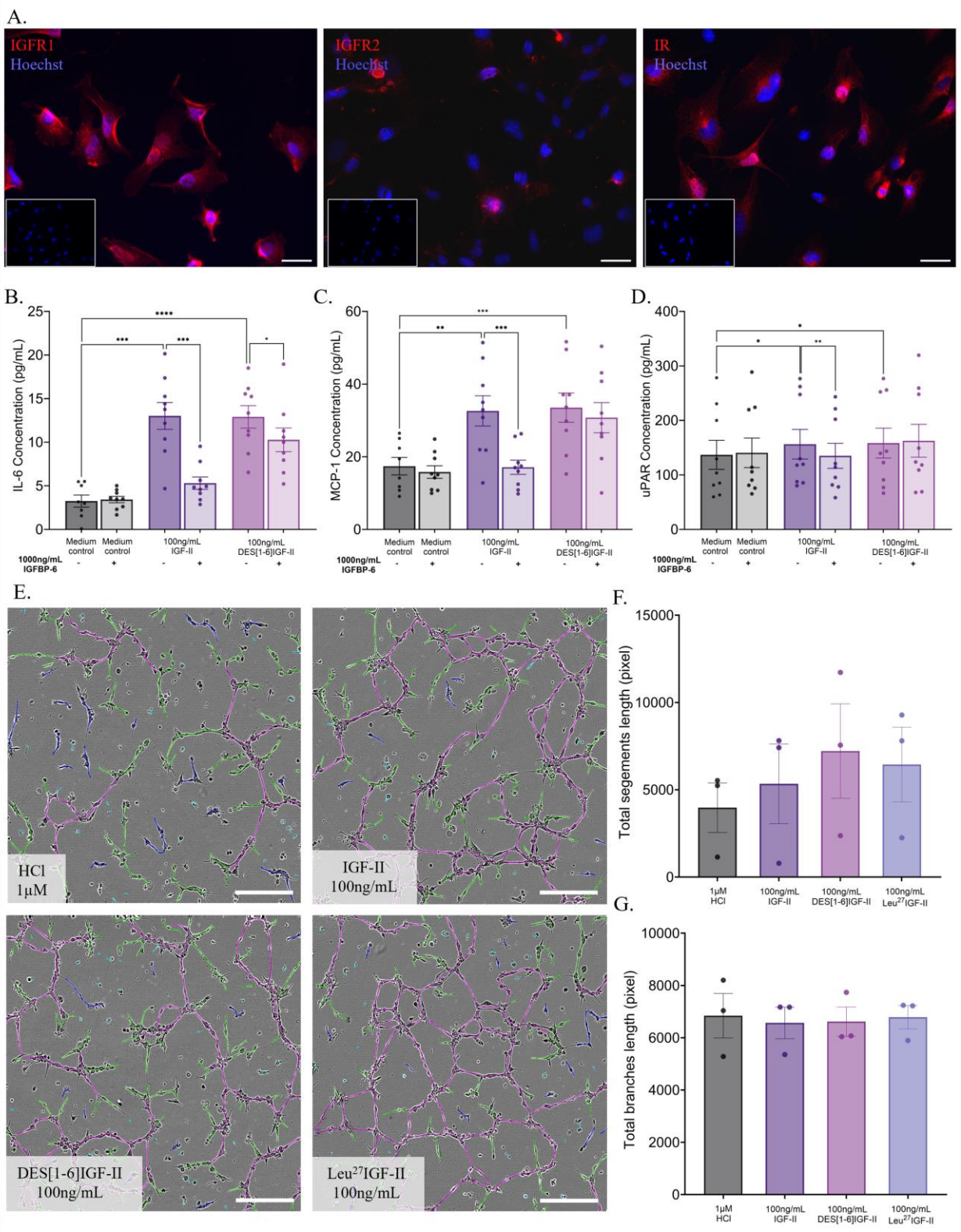

Figure 3 – **IGF-II Tends to Stimulate Angiogenesis *In Vitro*. A.** Representative images of immunocytochemistry staining show the presence of the three IGF-II receptors – IGFR1 (left panel), IGFR2 (middle panel), and IR (right panel) - on HMEC-1 endothelial cells. Nuclei were counterstained with Hoechst (blue). Insert shows the negative control. Scale bar represents 30µm. **B-D.** Semi-

Fig 3 – Continued
quantitative results from ELISA assays measuring three angiogenic factors: **B.** IL-6, **C.** MCP-1, and **D.** uPAR. ELISAs were conducted on conditioned media of HMEC-1 cells (n = 9 with 3 replicates) treated with 100 ng/mL IGF-II and DES[1-6]IGF-II. Both IGF variants stimulated the secretion of these angiogenic factors by HMEC-1 cells. The addition of IGFBP6 reduced the effects of IGF-II on the secretion of all three angiogenic factors and also diminished the effect of DES[1-6]IGF-II on IL-6 secretion by HMEC-1 cells. **E.** Representative images from the tube formation assay after 6 hours on HMEC-1 cells treated with 100 ng/mL of each IGF variant and their corresponding HCl control. The images display common parameters indicative of angiogenesis, including segments (magenta) and branches (green). Isolated elements (blue) and twigs (cyan) were not analysed. Scale bar represents 100µm. **F and G.** The effect of IGF variants on the total segment length and total branch length in the tube formation assay after 6 hours. Although neither IGF variant significantly stimulated total segment length, a positive trend is visible. Neither IGF stimulated total branch length. Data are expressed as mean ± SEM. N = 3 with 2-3 replicates per condition. Each data point represents an independent assay. *p<0,05; **p<0,01; ***p<0,001; ****p<0,0001. Statistical analysis was performed using mixed-effect analysis or RM one-way ANOVA with Dunnett's post hoc test or the non-parametric Friedmann test with Dunn's post hoc test to compare three or more groups. A paired t-test was performed to compare two groups. *ELISA, Enzyme-Linked Immune Sorbent Assay HCl, hydrochloric acid; HMEC-1, human microvascular endothelial cells; IGF, insulin-like growth factor; IGFR1, insulin-like growth factor receptor type 1; IGFR2, insulin-like growth factor receptor type 2; IL-6, interleukin 6; IR, insulin receptor; MCP-1, monocyte chemoattractant protein-1; RM, repeated measures; SEM, standard error of the mean; uPAR, urokinase plasminogen activator surface receptor*

DISCUSSION

Currently, ischemic stroke is one of the leading causes of death worldwide. Despite extensive research over the last couple of decades, treatment options remain limited. The inability of current therapies to repair and regenerate the damaged brain tissue results in life-altering consequences for stroke patients. Recently, there has been a growing consensus that stimulating the brain's endogenous repair mechanisms, particularly neurogenesis and angiogenesis, is crucial for improving long-term outcomes in stroke patients. The present study provides comprehensive insights into the role of IGF-II in neurogenesis, particularly focusing on the proliferation and migration of NSC, which are curial components of neurogenesis. This intricate process is essential for ischemic stroke recovery as it involves the generation of new neurons and their integration into existing neural networks (11). As this study demonstrated the presence of the three IGF-II receptors on NSC, it establishes the basis for the mechanistic effects of IGF-II. This research found that IGF-II and DES[1-6]IGF-II both stimulated the proliferation of NSC. A study by Ziegler *et al.* demonstrated that IGF-II was more potent in promoting NSC expansion compared to IGF-I and their standard growth medium (47). On the other hand, Leu^{27}IGF-II did not seem to have a stimulative effect on NSC proliferation. Leu^{27}IGF-II is a mutant form of IGF-II that binds to the IGFR2 but has a 20-fold reduction in binding to the IGFR1 (54). This finding could point us toward identifying which receptor could be involved in this process. Morrione *et al.* demonstrated that IGF-II induces cell proliferation by both the IGFR1 and the IR (55). A recent study described that IR isoform A (IR-A) is mainly responsible for the IGF-II-mediated proliferation of murine NSC (56). Future research, working with antibodies or small interfering RNA (siRNA) to block specific receptors, can validate the receptor involved in NSC proliferation. Additionally, it is noteworthy to mention that cell confluence was used as a measure of proliferation. However, more precise proliferation assays exist that utilise the principle of incorporating a substance (e.g. EdU or BrdU) during cell proliferation, which can be accurately quantified.

Following brain injury, such as ischemia, neural progenitor cells migrate into the injured regions, attempting differentiation and repair (57). Given the importance of NSC migration, this study implemented two distinct migration assays to assess the potential effect of IGF-II on NSC migration. The scratch-wound-healing assay investigated whether IGF-II would have direct effects on NSC migration. We found that IGF-II did not significantly increase NSC migration compared to their HCl control. Strikingly, IGF-II at 10 ng/mL significantly reduced migration of NSC. To the best of our knowledge, a scratch-wound-healing assay on NSC has not been described in the literature before. This assay also requires optimization, particularly in selecting the appropriate medium for NSC. The current scratch medium contained a reduced amount of growth factors and supplements, which may result in NSC survival rather than active migration. We further investigated NSC migration using a transwell migration assay. This assay was conducted to evaluate the chemotactic potential of

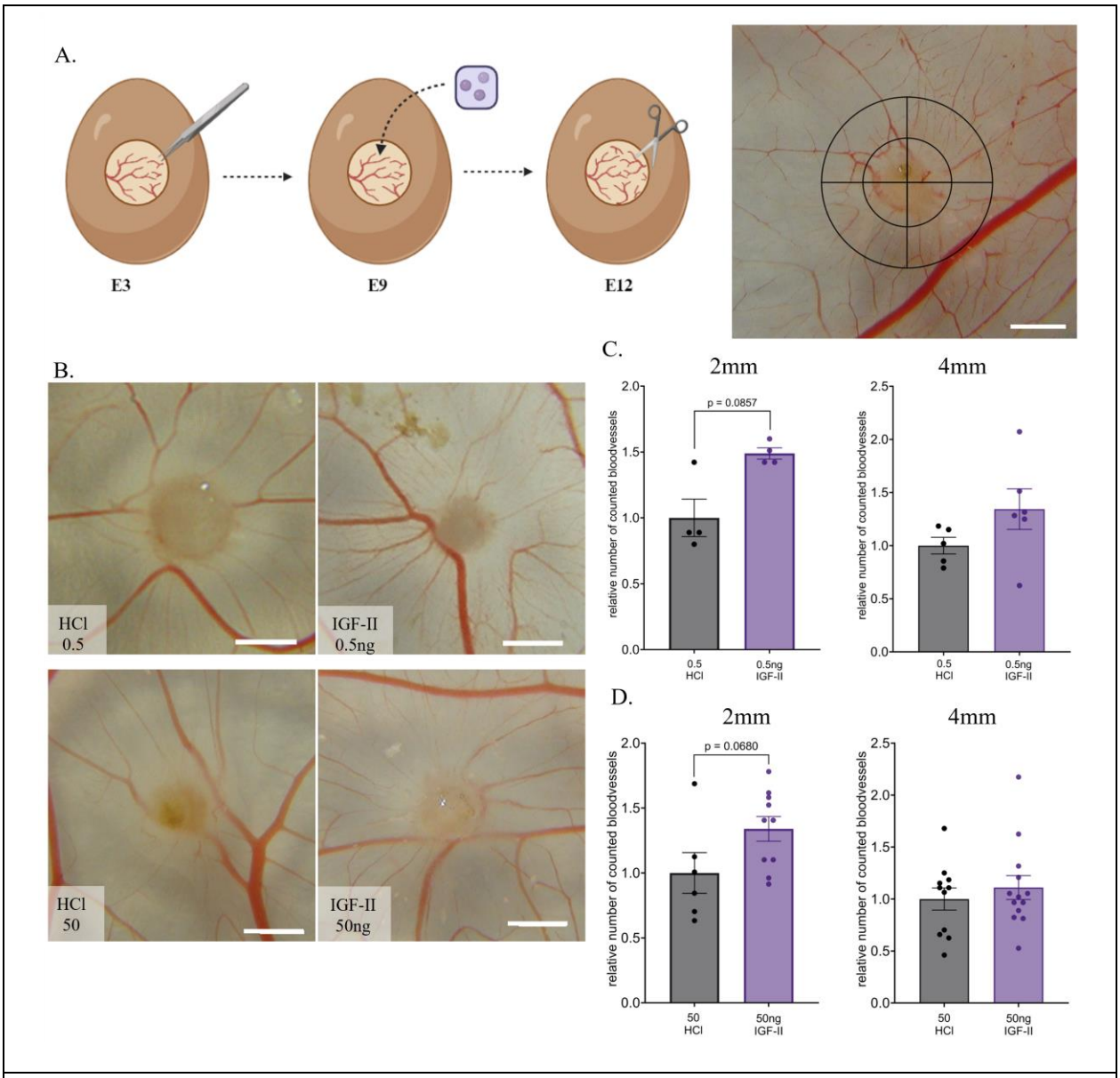

Figure 4 – IGF-II Tends to Induce Angiogenesis *In Ovo* via The CAM Assay. A. Schematic overview of the CAM assay (left panel). On embryonic day 3 (E3), a window was created by removing the eggshell. At E9, gelatin-absorbent sponges containing test conditions were placed on the CAM and incubated until E12. At E12, the CAM was isolated and photographed. Two concentric circles were digitally placed onto the CAM to count blood vessels (right panel). Scale bar represents 1 mm. The figure was made with Biorender **B.** Representative images of the isolated CAM treated with IGF-II and HCl control. Scale bar represents 1 mm. **C and D.** The average number of intersecting blood vessels of IGF-II 0,5 ng (n = 4-6) and 50 ng (n = 10-13) relative to their HCl 0.5 (n = 4-5) and 50 (n = 6-11) control at 2 mm and 4 mm. IGF-II tends to stimulate angiogenesis at 2 mm in the CAM assay but not at 4 mm. Scale bar represents 1 mm. Data are expressed as mean ± SEM. Statistical analysis was performed using an unpaired t-test or the Mann Whitney test. *CAM, chick chorioallantoic membrane; HCl, hydrochloric acid; IGF, insulin-like growth factor; SEM, standard error of the mean;*

IGF-II. Various studies already highlighted the chemotactic potential of IGF-II on various cell types. It was described that IGF-II stimulated basophil migration via chemotaxis (58). This was also observed for endothelial progenitor cells (59). In line with our hypothesis, we found that both IGF-II and DES[1-6]IGF-II stimulated chemotactic NSC migration at 100 and 1000 ng/mL. However, Leu^{27}IGF-II did not seem to stimulate chemotactic migration. This postulates that the chemotactic property of IGF-II can possibly be exerted via the IGFR1 and the IR. However, future experiments

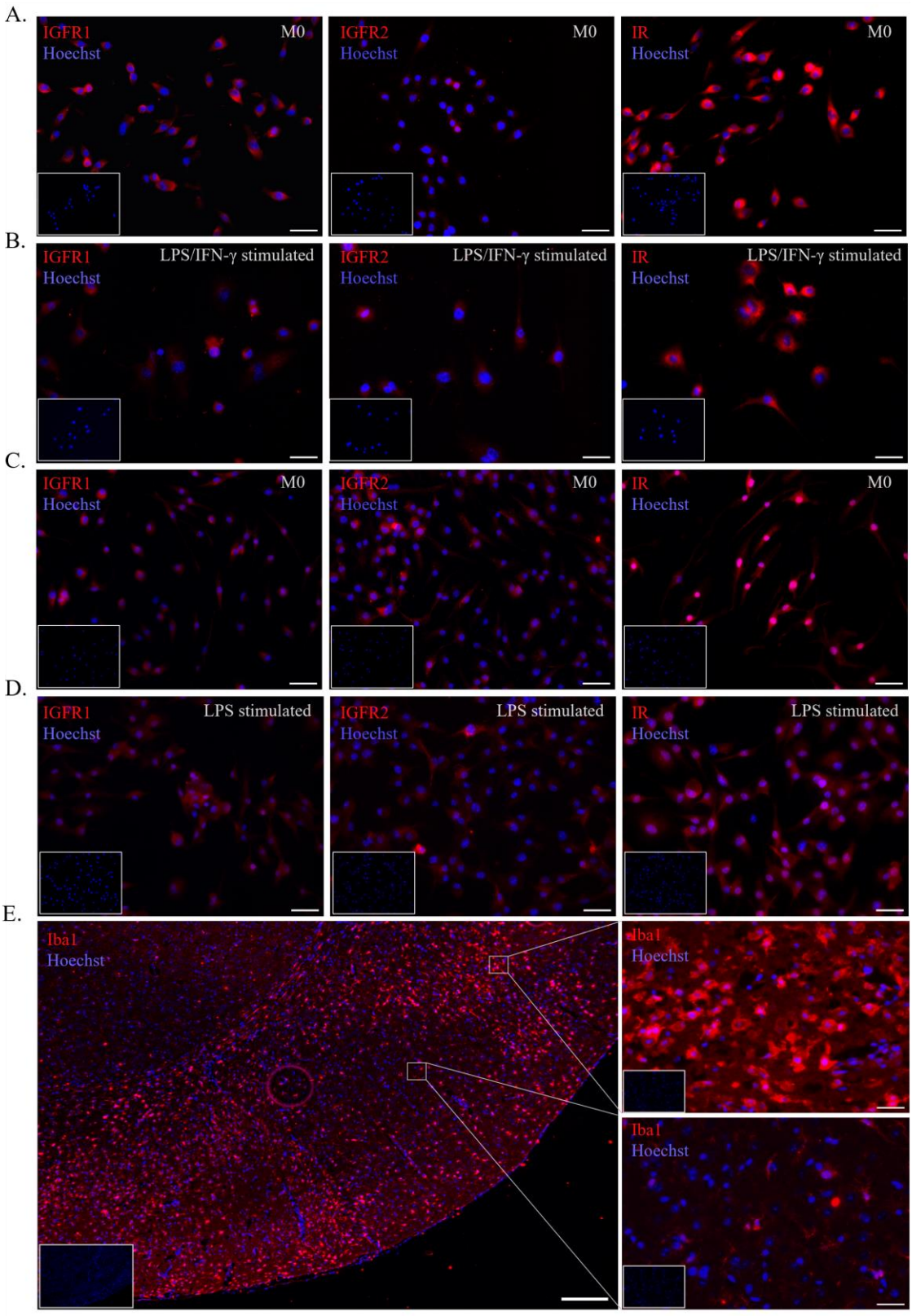

Figure 5 – IGF-II Can Potentially Be Neuroprotective By Acting On Macrophages. A-D. Representative immunocytochemistry staining of the three IGF-II receptors – IGFR1 (left panel), IGFR2 (middle panel) and IR (right panel) –

Figure 5 – Continued
on **A.** resting (M0) Raw264.7 cells, **B.** LPS/IFN-γ.-stimulated Raw264.7 cells, **C** resting (M0) BMDM and **D.** LPS/IFN-y stimulated BMDM. Scale bar represents 30µm. **E.** Representative images of immunofluorescent staining of a murine dMCAO brain coupe seven days post-stroke show the presence of Iba1 (red), which is expressed by macrophages and microglia (left panel). Scale bar represents 200 µm. At the border of the stroke area, Iba1 is highly expressed, indicating a large number of microglia and macrophages (right upper panel). In the stroke lesion area, Iba1 is less expressed, indicating a lower number of macrophages and microglia (right lower panel). Scale bar represents 30 µm. **A-E.** Nuclei were counterstained with Hoechst (blue). Insert shows the negative control. *BMDM, bone marrow-derived macrophages; dMCAO, distal middle cerebral artery occlusion; Iba1 ionized calcium-binding adaptor molecule 1; IFN-γ, interferon-gamma; IGFR1, insulin-like growth factor receptor type 1; IGFR2, insulin-like growth factor receptor type 2; IR, insulin receptor; LPS, lipopolysaccharide*

must validate this theory by selectively blocking specific IGF-II receptors. In addition, we hypothesised that the presence of IGFBP-6 would reduce the potency of IGF-II while the potency of DES[1-6]IGF-II remains. Surprisingly, at both tested concentrations, IGFBP-6 significantly reduced the chemotactic potency of DES[1-6]IGF-II and almost that of IGF-II. High variation and a relatively low number of biological replicates might explain these contradictory results, as IGF-II was close to being significantly reduced by IGFBP-6.

Beyond neurogenesis, another critical aspect of brain repair following ischemic stroke is angiogenesis. Key phases of angiogenesis consist of extracellular matrix (ECM) degradation, endothelial cell proliferation, migration, tube formation and vessel maturation (60). This study investigated the angiogenic potential of IGF-II *in vitro*. Many studies have already described the angiogenic properties of IGF-II on various aspects of angiogenesis (37, 61, 62). In previous studies from our research group, an angiogenesis antibody array was performed to investigate the angiogenic profile of IGF-II. From this angiogenesis antibody array, a few pro-angiogenic factors seemed to be upregulated, including IL-6, MCP-1 and uPAR. In this study, we confirmed that the conditioned media of IGF-II- or DES[1-6]IGF-II-treated HMEC-1 cells had an increased expression of these secreted angiogenic factors. Moreover, here, we could demonstrate that the presence of IGFBP-6 significantly reduced the effects of IGF-II for all three angiogenic factors, while the effects of DES[1-6]IGF-II were only reduced on IL-6 expression. These findings partially confirm our hypothesis that IGFBP-6 reduces the potency of IGF-II while that of DES[1-6]IGF-II primarily remains. As this study demonstrated increased expression of secreted angiogenic factors by IGF-II and DES[1-6]IGF-II-treated HMEC-1 cells, it was interesting to investigate if these IGFs would also induce tubelogenesis of HMEC-1 cells. A study by Lee *et al.* found that IGF-II could stimulate the tube formation of human umbilical vein endothelial cells (HUVEC), showing a clearly formed anastomosing capillary-like network (62). Although significantly enhanced tube formation could not be demonstrated in this study, a positive trend, however, is noticeable. HMEC-1 cells treated with IGF-II, DES[1-6]IGF-II or Leu^{27}IGF-II showed a visible increased anastomosing capillary-like network. No significance was obtained, but it should be noted that this could be due to a small sample size and the high variance, particularly when looking at the total segment length. In the future, this experiment must be repeated to ensure either stimulation or no stimulation of tube formation by IGF-II. A remarkable finding that stands out from the results reported earlier is that Leu^{27}IGF-II also displays a positive trend in stimulating tube formation, suggesting a role of the IGFR2 in angiogenesis. Several studies have already postulated that IGFR2 is involved in angiogenesis. Volpert *et al.* highlighted the necessity of IGFR2 to stimulate proliferin-induced migration of endothelial cells and to promote neovascularisation in the rat cornea (36). Moreover, their research demonstrated that both IGF-II and Leu^{27}IGF-II effectively stimulate endothelial cell migration and induce neovascularisation (36). Similarly, Herr *et al.* demonstrated that IGF-II stimulates uterine microvascular endothelial cells (UMVEC) migration and induces tube formation. They further established that the angiogenic potential of IGF-II is likely mediated via IGFR2, as the addition of antibodies against IGFR2 but not against IGFR1 or IR inhibited the IGF-II-induced tube formation (37). An important study by Maeng *et al.* found that locally generated IGF-II at ischemic sites may contribute to vasculogenesis by augmenting the recruitment of endothelial progenitor cells and that these effects are mediated via the IGFR2 (59).

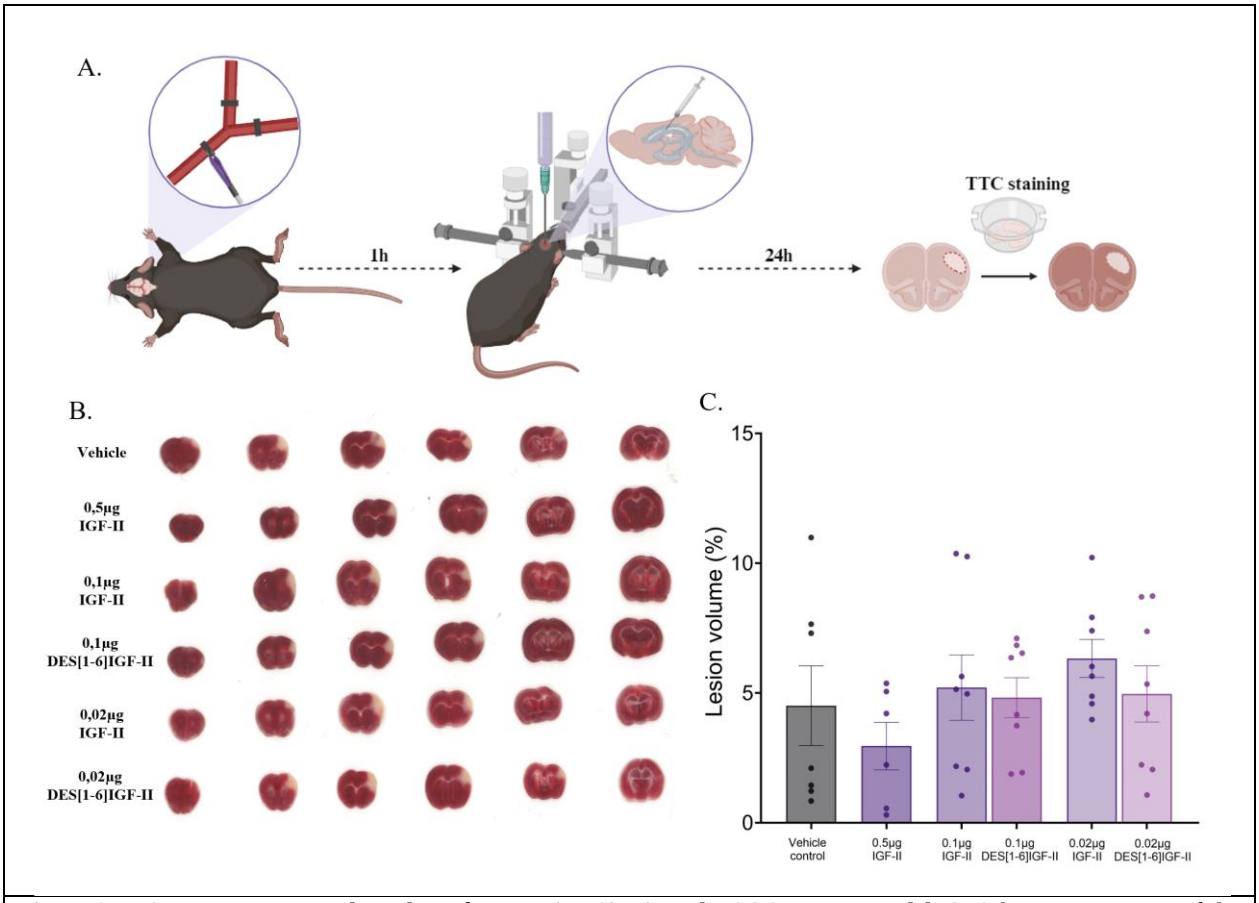

Figure 6 – IGF-II Does Not Reduce the Infarct Lesion Size in a dMCAO Mouse Model. A. Schematic overview of the experimental set-up. The dMCAO model was induced by occluding proximal and distal to the bifurcation of the middle cerebral artery (MCA). IGF-II treatment was given one hour after dMCAO inductions. Infarct volume was assessed 24 hours after dMCAO induction on brain coupes stained with TTC solution. The figure was made using Biorender. **B.** Representative images of TTC-stained brain coupes of C57BL/6 mice treated with various test conditions, showing the infarct lesion (white area). **C**. Quantification of the lesion volume of the different experimental groups (n = 6-8). Neither IGF-II nor DES[1-6]IGF-II at different concentrations reduced the infarct lesion volume. Data are expressed as mean ± SEM. Statistical analysis was performed using an ordinary one-way ANOVA with Dunnett's post hoc test. *dMCAO, distal middle cerebral artery occlusion; IGF, insulin-like growth factor; TTC, 2, 3, 5-triphenyltetrazolium chloride; SEM, standard error of the mean*

Altogether, these studies suggest that the angiogenic potential of IGF-II is mainly mediated through the IGFR2. However, the role of IGFR1 and IR in angiogenesis has also been described (63-65). Reinmuth *et al.* demonstrated that colon cancer cells transfected with a truncated dominant-negative form of IGFR1 resulted in decreased vascular endothelial growth factor (VEGF), a pro-angiogenic factor, expression (63). Moreover, Dallinga *et al.* identified IGF-II and IGFR1 as two novel tip cell-specific genes. Knockdown of both genes resulted in a decreased fraction of tip cells, the leading cells of sprouting, *in vitro* and *in vivo* (64). Finally, Walker *et al.* demonstrated that short hairpin RNA (shRNA)-mediated knockdown of the IR in HUVEC cells resulted in impaired VEGF signalling during angiogenic sprouting (65). Future research could validate the finding that Leu^{27}IGF-II could stimulate angiogenesis *in vitro* by repeating the tube formation assay, performing an HMEC-1 cell proliferation assay, and performing an angiogenesis antibody array. However, for now, our research provides us with an indication that the angiogenic potential of IGF-II could possibly be mediated via the IGFR2.

Another critical matter in the *in vitro* assessment of angiogenesis is the use of cell lines. In our study, we opted for HMEC-1 cells, a standard and widely used cell line for studying angiogenesis, as these cells retain many of the phenotypic and functional characteristics of primary endothelial cells (66). However, when

coupling back to ischemic stroke research, HMEC-1 cells alone may not provide a comprehensive understanding of brain angiogenesis during stroke recovery. To gain a more complete picture, it is beneficial also to include human brain microvascular endothelial cells (HBMEC) in future experiments. HBMEC cells are derived from the brain's microvasculature and accurately represent the endothelial cells from the BBB. Ischemic stroke directly affects the BBB, impairing its permeability and barrier function (6). Proper neuroregeneration during stroke recovery requires revascularisation in the brain, which ensures a functional and intact barrier to shield the brain against toxins and immune cells (67). Therefore, incorporating HBMEC cells in future studies can provide valuable insights into the effects of IGF-II on angiogenesis and BBB integrity during stroke recovery, thereby offering a more detailed understanding of its therapeutic potential. Additionally, to mimic the stroke environment *in vitro*, oxygen-glucose deprivation (OGD) conditions can also be introduced not only for HMEC-1 and HBMED cells but also when studying the NSC.

Furthermore, angiogenesis was assessed in an *in ovo* system via the CAM assay to gain more insights into the angiogenic potential of IGF-II. The CAM assay provides an accessible and more translational setting to study angiogenesis. As the chick is a living organism, this model provides a more physiological representative system for studying angiogenesis (68). This research showed that IGF-II tends to stimulate angiogenesis very locally. This suggests that IGF-II has paracrine effects, which enhance angiogenesis. Several other studies also confirmed the angiogenic potential of IGF-II with the CAM assay. In line with our results, Kim *et al.* also found that IGF-II stimulated vessel formation in the CAM assay (50). A study by Bae *et al.* indirectly determined angiogenic activity IGF-II. They used the conditioned media from hepatocellular carcinoma cells, which contained secreted IGF-II, and found that this media induced angiogenesis on the CAM (69). The CAM is an easy and cheap way to study angiogenesis in a more physiological and representative system. However, a few important limitations must be taken into account. The CAM on its own is very well vascularised; hence, distinguishing new capillaries from existing ones can be challenging (68). Additionally, developmental angiogenesis usually occurs until E11. Therefore, it is best to wait after E11 to obtain the results (68). To avoid this, we analysed the results on E12. In conclusion, our study provided valuable insights into the angiogenic properties of IGF-II by studying angiogenesis both *in vitro* and *in ovo*.

The present study contributes to our understanding of whether IGF-II can be neuroprotective by acting on macrophages. Neuroprotection involves mechanisms and cellular processes aimed at protecting the brain tissue from further damage and promoting its recovery (18). Neuroprotective properties of IGF-II have already been described in literature in various aspects, as well as various neurological disorders. However, this study focuses on macrophages and their potential to reduce neuroinflammation. Our study demonstrated the presence of all three IGF-II receptors on a macrophage cell line as well as on BMDMs. This study also detected the three receptors on LPS-stimulated macrophages, which display a pro-inflammatory state. Looking at pro-inflammatory macrophages is highly relevant for stroke research as macrophages migrate towards the ischemic lesion during the acute phase of stroke. There, they display a more pro-inflammatory state, increasing neuroinflammation and worsening stroke outcomes (13). By demonstrating the expression of the three IGF-II receptors on both resting macrophages and LPS-stimulated macrophages, it can be postulated that IGF-II can act on their spectrum of phenotypes. A study by Du *et al.* revealed that IGF-II can preprogram macrophages to become more anti-inflammatory during their maturation and that these macrophages alleviated EAE mice (44). Another study suggested that IGF-II exhibits dual opposing roles in determining the macrophage state (70). During macrophage maturation, binding to the IGFR2 endows IGF-II with the capability to induce an anti-inflammatory state in macrophages. On the contrary, IGFR1 activation leads to a more pro-inflammatory state (70). To the best of our knowledge, no studies have investigated the phenomenon of phenotype shifting in mature resting or pro-inflammatory macrophages induced by IGF-II. Not only macrophages contribute to neuroinflammation after ischemic stroke. Similar to macrophages, the brain resident microglia are considered to be neurotoxic during the acute phase

(5, 6). The presence of both activated macrophages and microglia in and near the stroke lesion was demonstrated in this study. Future studies on the effects of IGF-II on the phenotypic switch of macrophages and microglia will elucidate more about the neuroprotective potential of IGF-II. Investigating the expression of different pro and anti-inflammatory markers expressed by IGF-II-treated or untreated macrophages and microglia using FACS or qPCR will already give a clear first indication of the neuroprotective properties of IGF-II regarding neuroinflammation.

An *in vivo* experiment was conducted to provide an initial indication of the neuroprotective properties of IGF-II. Prior to the *in vivo* experiment, this study also demonstrated that IGF-II receptors are present in healthy brain tissue. Additionally, we demonstrated that three and seven days after stroke onset, IGF-II receptors are present in and near the stroke lesion. However, it seems that different receptors are upregulated at different time points. In healthy brain tissue, it seems that IGFR1 and IR are primarily expressed, while almost nothing is observed from the IGFR2. Three days after stroke onset, the IGFR2 receptor seems to be upregulated compared to the healthy brain tissue, while IGFR1 and IR also seem to show less expression. Finally, seven days after stroke onset, both IGFR1 and IR receptors were observed to be upregulated again, while IGFR2 showed very little presence. Perhaps different activated processes related to ischemic stroke recovery require upregulating specific IGF-II receptors at different time points. In line with our results, IR and IGFR1 are widely expressed in the healthy brain with specific, more dense regions (29, 71). Despite our contradictory results, some studies detected IGFR2 expression in healthy murine brain tissue (72, 73). For our study, careful consideration of this data must be taken because the antibodies used for IF staining were not validated for IF with paraffin coupes. Whether the antibodies failed to work or we actually observed differential receptor expression must definitely be further investigated. A simple qPCR and western blot on healthy and stroke brain tissue can easily provide quantitative results of receptor expression on both mRNA and protein levels. As the presence of some IGF-II receptors was detected in dMCAO stroke brain tissue, it was expected that IGF-II or DES[1-6]IGF-II might reduce the infarct lesion size. However, we found that treatment with either IGF-II or DES[1-6]IGF-II did not reduce the infarct lesion size in a dMCAO mouse model. The administered dose of IGF-II and DES[1-6]IGF-II was based on literature, and by previous experiments from our research group, it was found that the lowest concentration of IGF-II (0.5 µg) was the most effective. It was decided to lower the dose of both IGFs to investigate whether an even lower dose would exhibit better effects. Possibly, the dose was suboptimal and inefficient in inducing neuroprotective effects. Additionally, a considerable variation within mice of the same treatment group can also explain the insignificant effect. In a dMCAO model, electrocoagulation occurs proximal and distal to the bifurcation of the middle cerebral artery (53). However, anatomical variations in this bifurcation point exist, leading to small variations in the actual electrocoagulation (53). The dMCAO model has become the most frequently used animal model in experimental stroke research and is considered to be highly representative of human ischemic stroke conditions (74). The resulting infarct volume and localisation after dMCAO coagulation corresponds to the ischemic brain lesions in the majority of human strokes in proportion to brain size (53, 75). In our study, we used 10-week-old male mice, which is usually the population of mice used for a proof-of-principle. According to the Stroke Therapy Academic Industry Roundtable (STAIR) guidelines, stroke research should be reproducible in various models (76, 77). So, exploring the effects on female mice, older mice or mice with comorbidities representative of human populations, including hypertension and diabetes, must also be thoroughly investigated. An additional STAIR recommendation is that a positive result from a drug study must always be verified in another species and should also be replicable in a further stroke model (76, 77). The dMCAO model is a form of permanent occlusion, however, the effects of IGF-II must also be studied in a transient occlusion model. A great example of a transient model is the monofilament model or the intraluminal suture MCAO model. In this model, a suture is introduced directly into the internal carotid artery, and the suture is advanced until it interrupts the blood supply to the MCA (78). This model enables both permanent and transient ischemia, thereby allowing the evaluation of the neuroprotective effects of IGF-II under different ischemic conditions.

In the future, it will also be useful to explore other routes of administration of the IGF-II treatment. In general, stereotactical injection into the ventricles allows researchers to control the location and dose of the administered drug precisely (79). However, when translating this to the clinic, it is too invasive and the potential benefits would not outweigh the inherent risks of the procedure. Therefore, other routes can be explored in future *in vivo* experiments. Different routes of administration can be used by making use of the ability of circulating IGFs to cross fenestrated and sinusoidal capillaries as well as the BBB (80-82). Moreover, as for ischemic stroke, where the BBB permeability is increased, IGF-II can likely cross the BBB without difficulty (83). Subcutaneous administration of IGF-II could be a safe and practical route, and indeed, several studies already confirmed the positive effects of subcutaneously administered IGF-II (80, 84, 85). Additionally, one study demonstrated memory enhancement after systemic administration of IGF-II (86). A potential issue with the subcutaneous route is that BBB-related IGF-II transport can be impaired in stroke. The bioavailability of subcutaneously administered IGF-II to the brain may be enhanced or reduced (80). So, researchers are unable to control the exact doses that actually reach the brain or the stroke lesion area. Intranasal delivery can circumvent this potential issue of subcutaneous administration as this route bypasses the BBB (87). Once in the brain, substances are distributed deeper into the brain (87). Only one study, by Pardo *et al.*, was found that uses IGF-II intranasally. They demonstrated that intranasal IGF-II ameliorated siRNA-induced cognitive impairments (88). Future research will determine the optimal administration route for IGF-II, balancing safety and therapeutic efficacy.

In general, IGF-II, DES[1-6]IGF-II and Leu^{27}IGF-II were diluted in HCl (pH = 2). This solution on its own can be harsh for the cells both *in vitro* and *in vivo*. The manufacturer recommended dissolving the IGFs in HCl to ensure they adopted the optimal structural conformation for maximal effectiveness. In clinical settings, using a strong acid may cause safety issues. Bioinformatics can be used to identify further potential solvents that can effectively solubilise IGF-II while maintaining its optimal structural conformation and ensuring safety for clinical use.

CONCLUSION

In conclusion, ischemic stroke remains a major global health concern, necessitating innovative therapeutic strategies to improve patient outcomes. Recent extensive research emphasises the importance of harnessing endogenous repair mechanisms, including neurogenesis and angiogenesis, for effective stroke recovery. Our research provided comprehensive insights into the role of IGF-II in relation to these processes. Briefly, this study demonstrated IGF-II's neuroregenerative potential as it stimulated key processes of neurogenesis and exhibited angiogenic properties. This study also postulated the involvement of the different receptors in these activated processes. Furthermore, the first indication of possible neuroprotective capacities was demonstrated to broaden the therapeutic potential of IGF-II. In summary, our study contributes to a deeper understanding of the multifaceted roles of IGF-II in stroke recovery mechanisms. Our research provides valuable insights for developing novel therapeutic strategies targeting neurogenesis, angiogenesis, and neuroinflammation in ischemic stroke. Further research is necessary to validate these findings and optimise the therapeutic potential of IGF-II for clinical translation.

REFERENCES

1. Campbell BCV, De Silva DA, Macleod MR, Coutts SB, Schwamm LH, Davis SM, et al. Ischaemic stroke. Nat Rev Dis Primers. 2019;5(1):70.
2. Tadi P, Lui F. Acute Stroke. StatPearls. Treasure Island (FL)2023.
3. Kuriakose D, Xiao Z. Pathophysiology and Treatment of Stroke: Present Status and Future Perspectives. Int J Mol Sci. 2020;21(20).
4. Pu L, Wang L, Zhang R, Zhao T, Jiang Y, Han L. Projected Global Trends in Ischemic Stroke Incidence, Deaths and Disability-Adjusted Life Years From 2020 to 2030. Stroke. 2023;54(5):1330-9.
5. Xing C, Arai K, Lo EH, Hommel M. Pathophysiologic cascades in ischemic stroke. Int J Stroke. 2012;7(5):378-85.
6. Woodruff TM, Thundyil J, Tang SC, Sobey CG, Taylor SM, Arumugam TV. Pathophysiology, treatment, and animal and cellular models of human ischemic stroke. Mol Neurodegener. 2011;6(1):11.
7. MartInez-Coria H, Arrieta-Cruz I, Cruz ME, Lopez-Valdes HE. Physiopathology of ischemic stroke and its modulation using memantine: evidence from preclinical stroke. Neural Regen Res. 2021;16(3):433-9.
8. Belov Kirdajova D, Kriska J, Tureckova J, Anderova M. Ischemia-Triggered Glutamate Excitotoxicity From the Perspective of Glial Cells. Front Cell Neurosci. 2020;14:51.
9. Mehta SL, Manhas N, Raghubir R. Molecular targets in cerebral ischemia for developing novel therapeutics. Brain Res Rev. 2007;54(1):34-66.
10. Jurcau A, Ardelean AI. Oxidative Stress in Ischemia/Reperfusion Injuries following Acute Ischemic Stroke. Biomedicines. 2022;10(3).
11. Dillen Y, Kemps H, Gervois P, Wolfs E, Bronckaers A. Adult Neurogenesis in the Subventricular Zone and Its Regulation After Ischemic Stroke: Implications for Therapeutic Approaches. Transl Stroke Res. 2020;11(1):60-79.
12. Abdullahi W, Tripathi D, Ronaldson PT. Blood-brain barrier dysfunction in ischemic stroke: targeting tight junctions and transporters for vascular protection. Am J Physiol Cell Physiol. 2018;315(3):C343-C56.
13. Ponsaerts L, Alders L, Schepers M, de Oliveira RMW, Prickaerts J, Vanmierlo T, et al. Neuroinflammation in Ischemic Stroke: Inhibition of cAMP-Specific Phosphodiesterases (PDEs) to the Rescue. Biomedicines. 2021;9(7).
14. Jayaraj RL, Azimullah S, Beiram R, Jalal FY, Rosenberg GA. Neuroinflammation: friend and foe for ischemic stroke. J Neuroinflammation. 2019;16(1):142.
15. Planas AM. Role of Immune Cells Migrating to the Ischemic Brain. Stroke. 2018;49(9):2261-7.
16. Hurd MD, Goel I, Sakai Y, Teramura Y. Current status of ischemic stroke treatment: From thrombolysis to potential regenerative medicine. Regen Ther. 2021;18:408-17.
17. Jovin TG, Chamorro A, Cobo E, de Miquel MA, Molina CA, Rovira A, et al. Thrombectomy within 8 hours after symptom onset in ischemic stroke. N Engl J Med. 2015;372(24):2296-306.
18. Haupt M, Gerner ST, Bahr M, Doeppner TR. Neuroprotective Strategies for Ischemic Stroke-Future Perspectives. Int J Mol Sci. 2023;24(5).
19. Jiao Y, Liu YW, Chen WG, Liu J. Neuroregeneration and functional recovery after stroke: advancing neural stem cell therapy toward clinical application. Neural Regen Res. 2021;16(1):80-92.
20. Zhang R, Zhang Z, Wang L, Wang Y, Gousev A, Zhang L, et al. Activated neural stem cells contribute to stroke-induced neurogenesis and neuroblast migration toward the infarct boundary in adult rats. J Cereb Blood Flow Metab. 2004;24(4):441-8.
21. Arvidsson A, Collin T, Kirik D, Kokaia Z, Lindvall O. Neuronal replacement from endogenous precursors in the adult brain after stroke. Nat Med. 2002;8(9):963-70.
22. Jin K, Sun Y, Xie L, Peel A, Mao XO, Batteur S, et al. Directed migration of neuronal precursors into the ischemic cerebral cortex and striatum. Mol Cell Neurosci. 2003;24(1):171-89.
23. Rahman AA, Amruta N, Pinteaux E, Bix GJ. Neurogenesis After Stroke: A Therapeutic Perspective. Transl Stroke Res. 2021;12(1):1-14.
24. Rust R. Insights into the dual role of angiogenesis following stroke. J Cereb Blood Flow Metab. 2020;40(6):1167-71.
25. Nih LR, Gojgini S, Carmichael ST, Segura T. Dual-function injectable angiogenic biomaterial for the repair of brain tissue following stroke. Nat Mater. 2018;17(7):642-51.
26. Rust R, Gronnert L, Gantner C, Enzler A, Mulders G, Weber RZ, et al. Nogo-A targeted therapy promotes vascular repair and functional recovery following stroke. Proc Natl Acad Sci U S A. 2019;116(28):14270-9.
27. Hong JM, Choi MH, Park GH, Shin HS, Lee SJ, Lee JS, et al. Transdural Revascularization by Multiple Burrhole After Erythropoietin in Stroke Patients With Cerebral Hypoperfusion: A Randomized Controlled Trial. Stroke. 2022;53(9):2739-48.
28. Rajpathak SN, Gunter MJ, Wylie-Rosett J, Ho GY, Kaplan RC, Muzumdar R, et al. The role of insulin-like growth factor-I and its binding proteins in glucose homeostasis and type 2 diabetes. Diabetes Metab Res Rev. 2009;25(1):3-12.
29. Werner H, LeRoith D. Insulin and insulin-like growth factor receptors in the brain: physiological and pathological aspects. Eur Neuropsychopharmacol. 2014;24(12):1947-53.

30. O'Kusky J, Ye P. Neurodevelopmental effects of insulin-like growth factor signaling. Front Neuroendocrinol. 2012;33(3):230-51.
31. Benarroch EE. Insulin-like growth factors in the brain and their potential clinical implications. Neurology. 2012;79(21):2148-53.
32. Blyth AJ, Kirk NS, Forbes BE. Understanding IGF-II Action through Insights into Receptor Binding and Activation. Cells. 2020;9(10).
33. Glasser AL, Boudeau J, Barnich N, Perruchot MH, Colombel JF, Darfeuille-Michaud A. Adherent invasive Escherichia coli strains from patients with Crohn's disease survive and replicate within macrophages without inducing host cell death. Infect Immun. 2001;69(9):5529-37.
34. Selenou C, Brioude F, Giabicani E, Sobrier ML, Netchine I. IGF2: Development, Genetic and Epigenetic Abnormalities. Cells. 2022;11(12).
35. LeRoith D, Holly JMP, Forbes BE. Insulin-like growth factors: Ligands, binding proteins, and receptors. Mol Metab. 2021;52:101245.
36. Volpert O, Jackson D, Bouck N, Linzer DI. The insulin-like growth factor II/mannose 6-phosphate receptor is required for proliferin-induced angiogenesis. Endocrinology. 1996;137(9):3871-6.
37. Herr F, Liang OD, Herrero J, Lang U, Preissner KT, Han VK, et al. Possible angiogenic roles of insulin-like growth factor II and its receptors in uterine vascular adaptation to pregnancy. J Clin Endocrinol Metab. 2003;88(10):4811-7.
38. Menuelle P, Babajko S, Plas C. Insulin-like growth factor (IGF) binding proteins modulate the glucocorticoid-dependent biological effects of IGF-II in cultured fetal rat hepatocytes. Endocrinology. 1999;140(5):2232-40.
39. Bach LA. Current ideas on the biology of IGFBP-6: More than an IGF-II inhibitor? Growth Horm IGF Res. 2016;30-31:81-6.
40. Francis GL, Aplin SE, Milner SJ, McNeil KA, Ballard FJ, Wallace JC. Insulin-like growth factor (IGF)-II binding to IGF-binding proteins and IGF receptors is modified by deletion of the N-terminal hexapeptide or substitution of arginine for glutamate-6 in IGF-II. Biochem J. 1993;293 (Pt 3)(Pt 3):713-9.
41. GroPep. Human DES[1-6]IGF-II [Available from: https://gropep.com/product/human-des-1-6-igf-ii/.
42. Guler HP, Zapf J, Schmid C, Froesch ER. Insulin-like growth factors I and II in healthy man. Estimations of half-lives and production rates. Acta Endocrinol (Copenh). 1989;121(6):753-8.
43. Guo D, Xu Y, Liu Z, Wang Y, Xu X, Li C, et al. IGF2 inhibits hippocampal over-activated microglia and alleviates depression-like behavior in LPS- treated male mice. Brain Res Bull. 2023;194:1-12.
44. Du L, Lin L, Li Q, Liu K, Huang Y, Wang X, et al. IGF-2 Preprograms Maturing Macrophages to Acquire Oxidative Phosphorylation-Dependent Anti-inflammatory Properties. Cell Metab. 2019;29(6):1363-75 e8.
45. Bracko O, Singer T, Aigner S, Knobloch M, Winner B, Ray J, et al. Gene expression profiling of neural stem cells and their neuronal progeny reveals IGF2 as a regulator of adult hippocampal neurogenesis. J Neurosci. 2012;32(10):3376-87.
46. Lehtinen MK, Zappaterra MW, Chen X, Yang YJ, Hill AD, Lun M, et al. The cerebrospinal fluid provides a proliferative niche for neural progenitor cells. Neuron. 2011;69(5):893-905.
47. Ziegler AN, Schneider JS, Qin M, Tyler WA, Pintar JE, Fraidenraich D, et al. IGF-II promotes stemness of neural restricted precursors. Stem Cells. 2012;30(6):1265-76.
48. Hartnett L, Glynn C, Nolan CM, Grealy M, Byrnes L. Insulin-like growth factor-2 regulates early neural and cardiovascular system development in zebrafish embryos. Int J Dev Biol. 2010;54(4):573-83.
49. Kondo T, Vicent D, Suzuma K, Yanagisawa M, King GL, Holzenberger M, et al. Knockout of insulin and IGF-1 receptors on vascular endothelial cells protects against retinal neovascularization. J Clin Invest. 2003;111(12):1835-42.
50. Kim KW, Bae SK, Lee OH, Bae MH, Lee MJ, Park BC. Insulin-like growth factor II induced by hypoxia may contribute to angiogenesis of human hepatocellular carcinoma. Cancer Res. 1998;58(2):348-51.
51. Gervois P, Ratajczak J, Wolfs E, Vangansewinkel T, Dillen Y, Merckx G, et al. Preconditioning of Human Dental Pulp Stem Cells with Leukocyte- and Platelet-Rich Fibrin-Derived Factors Does Not Enhance Their Neuroregenerative Effect. Stem Cells Int. 2019;2019:8589149.
52. Carpentier G, Berndt S, Ferratge S, Rasband W, Cuendet M, Uzan G, et al. Angiogenesis Analyzer for ImageJ - A comparative morphometric analysis of "Endothelial Tube Formation Assay" and "Fibrin Bead Assay". Sci Rep. 2020;10(1):11568.
53. Llovera G, Roth S, Plesnila N, Veltkamp R, Liesz A. Modeling stroke in mice: permanent coagulation of the distal middle cerebral artery. J Vis Exp. 2014(89):e51729.
54. GroPep. Human [Leu27]IGF-II [Available from: https://gropep.com/product/human-leu27-igf-ii/.
55. Morrione A, Valentinis B, Xu SQ, Yumet G, Louvi A, Efstratiadis A, et al. Insulin-like growth factor II stimulates cell proliferation through the insulin receptor. Proc Natl Acad Sci U S A. 1997;94(8):3777-82.
56. Ziegler AN, Chidambaram S, Forbes BE, Wood TL, Levison SW. Insulin-like growth factor-II (IGF-II) and IGF-II analogs with enhanced insulin receptor-a

binding affinity promote neural stem cell expansion. J Biol Chem. 2014;289(8):4626-33.
57. Motamed S, Del Borgo MP, Zhou K, Kulkarni K, Crack PJ, Merson TD, et al. Migration and Differentiation of Neural Stem Cells Diverted From the Subventricular Zone by an Injectable Self-Assembling beta-Peptide Hydrogel. Front Bioeng Biotechnol. 2019;7:315.
58. Hartnell A, Heinemann A, Conroy DM, Wait R, Sturm GJ, Caversaccio M, et al. Identification of selective basophil chemoattractants in human nasal polyps as insulin-like growth factor-1 and insulin-like growth factor-2. J Immunol. 2004;173(10):6448-57.
59. Maeng YS, Choi HJ, Kwon JY, Park YW, Choi KS, Min JK, et al. Endothelial progenitor cell homing: prominent role of the IGF2-IGF2R-PLCbeta2 axis. Blood. 2009;113(1):233-43.
60. Merckx G, Hosseinkhani B, Kuypers S, Deville S, Irobi J, Nelissen I, et al. Angiogenic Effects of Human Dental Pulp and Bone Marrow-Derived Mesenchymal Stromal Cells and their Extracellular Vesicles. Cells. 2020;9(2).
61. Kim JH, Park SW, Yu YS, Kim KW, Kim JH. Hypoxia-induced insulin-like growth factor II contributes to retinal vascularization in ocular development. Biochimie. 2012;94(3):734-40.
62. Lee OH, Bae SK, Bae MH, Lee YM, Moon EJ, Cha HJ, et al. Identification of angiogenic properties of insulin-like growth factor II in in vitro angiogenesis models. Br J Cancer. 2000;82(2):385-91.
63. Reinmuth N, Fan F, Liu W, Parikh AA, Stoeltzing O, Jung YD, et al. Impact of insulin-like growth factor receptor-I function on angiogenesis, growth, and metastasis of colon cancer. Lab Invest. 2002;82(10):1377-89.
64. Dallinga MG, Yetkin-Arik B, Kayser RP, Vogels IMC, Nowak-Sliwinska P, Griffioen AW, et al. IGF2 and IGF1R identified as novel tip cell genes in primary microvascular endothelial cell monolayers. Angiogenesis. 2018;21(4):823-36.
65. Walker AMN, Warmke N, Mercer B, Watt NT, Mughal R, Smith J, et al. Endothelial Insulin Receptors Promote VEGF-A Signaling via ERK1/2 and Sprouting Angiogenesis. Endocrinology. 2021;162(8).
66. Cytion.com. HMEC-1 Cells [Available from: https://www.cytion.com/HMEC-1-Cells/304064.
67. Pong S, Karmacharya R, Sofman M, Bishop JR, Lizano P. The Role of Brain Microvascular Endothelial Cell and Blood-Brain Barrier Dysfunction in Schizophrenia. Complex Psychiatry. 2020;6(1-2):30-46.
68. Staton CA, Reed MW, Brown NJ. A critical analysis of current in vitro and in vivo angiogenesis assays. Int J Exp Pathol. 2009;90(3):195-221.
69. Bae MH, Lee MJ, Bae SK, Lee OH, Lee YM, Park BC, et al. Insulin-like growth factor II (IGF-II) secreted from HepG2 human hepatocellular carcinoma cells shows angiogenic activity. Cancer Lett. 1998;128(1):41-6.
70. Wang X, Lin L, Lan B, Wang Y, Du L, Chen X, et al. IGF2R-initiated proton rechanneling dictates an anti-inflammatory property in macrophages. Sci Adv. 2020;6(48).
71. Alata W, Yogi A, Brunette E, Delaney CE, van Faassen H, Hussack G, et al. Targeting insulin-like growth factor-1 receptor (IGF1R) for brain delivery of biologics. FASEB J. 2022;36(3):e22208.
72. Ocrant I, Valentino KL, Eng LF, Hintz RL, Wilson DM, Rosenfeld RG. Structural and immunohistochemical characterization of insulin-like growth factor I and II receptors in the murine central nervous system. Endocrinology. 1988;123(2):1023-34.
73. Gammeltoft S, Haselbacher GK, Humbel RE, Fehlmann M, Van Obberghen E. Two types of receptor for insulin-like growth factors in mammalian brain. EMBO J. 1985;4(13A):3407-12.
74. Howells DW, Porritt MJ, Rewell SS, O'Collins V, Sena ES, van der Worp HB, et al. Different strokes for different folks: the rich diversity of animal models of focal cerebral ischemia. J Cereb Blood Flow Metab. 2010;30(8):1412-31.
75. Carmichael ST. Rodent models of focal stroke: size, mechanism, and purpose. NeuroRx. 2005;2(3):396-409.
76. Lapchak PA, Zhang JH, Noble-Haeusslein LJ. RIGOR guidelines: escalating STAIR and STEPS for effective translational research. Transl Stroke Res. 2013;4(3):279-85.
77. Fisher M, Feuerstein G, Howells DW, Hurn PD, Kent TA, Savitz SI, et al. Update of the stroke therapy academic industry roundtable preclinical recommendations. Stroke. 2009;40(6):2244-50.
78. Fluri F, Schuhmann MK, Kleinschnitz C. Animal models of ischemic stroke and their application in clinical research. Drug Des Devel Ther. 2015;9:3445-54.
79. Landeck N, Conti Mazza M, Duffy M, Bishop C, Sortwell CE, Cookson MR. Stereotaxic Intracranial Delivery of Chemicals, Proteins or Viral Vectors to Study Parkinson's Disease. J Vis Exp. 2021(168).
80. Fitzgerald GS, Chuchta TG, McNay EC. Insulin-like growth factor-2 is a promising candidate for the treatment and prevention of Alzheimer's disease. CNS Neurosci Ther. 2023;29(6):1449-69.
81. Reinhardt RR, Bondy CA. Insulin-like growth factors cross the blood-brain barrier. Endocrinology. 1994;135(5):1753-61.
82. Lewitt MS, Boyd GW. Role of the Insulin-like Growth Factor System in Neurodegenerative Disease. Int J Mol Sci. 2024;25(8).
83. Mathias K, Machado RS, Stork S, Dos Santos D, Joaquim L, Generoso J, et al. Blood-brain barrier

permeability in the ischemic stroke: An update. Microvasc Res. 2024;151:104621.
84. Cruz E, Descalzi G, Steinmetz A, Scharfman HE, Katzman A, Alberini CM. CIM6P/IGF-2 Receptor Ligands Reverse Deficits in Angelman Syndrome Model Mice. Autism Res. 2021;14(1):29-45.
85. Zhuang HX, Snyder CK, Pu SF, Ishii DN. Insulin-like growth factors reverse or arrest diabetic neuropathy: effects on hyperalgesia and impaired nerve regeneration in rats. Exp Neurol. 1996;140(2):198-205.
86. Stern SA, Kohtz AS, Pollonini G, Alberini CM. Enhancement of memories by systemic administration of insulin-like growth factor II. Neuropsychopharmacology. 2014;39(9):2179-90.
87. Lochhead JJ, Davis TP. Perivascular and Perineural Pathways Involved in Brain Delivery and Distribution of Drugs after Intranasal Administration. Pharmaceutics. 2019;11(11).
88. Pardo M, Cheng Y, Velmeshev D, Magistri M, Eldar-Finkelman H, Martinez A, et al. Intranasal siRNA administration reveals IGF2 deficiency contributes to impaired cognition in Fragile X syndrome mice. JCI Insight. 2017;2(6):e91782.

This text was grammatically supported by GenAI

Acknowledgements – I would like to express my sincere gratitude to my daily supervisor, Lotte Alders, for providing the best guidance and support throughout this internship. I am also deeply grateful to my principal investigator, Prof. Dr. Annelies Bronckaers, for her exceptional mentorship. I am also very grateful to Sarah Vandebroek and Amber Van Bocxlaer for their great assistance with experiments and data analysis during their junior internship. My heartfelt thanks go to the Team LISSA members for their valuable input during meetings and for always helping out when needed. A special thanks to Dr. Florian Hermans for teaching me the skills to perform stainings, and a big thanks to Evelyne Vankerkove for providing the best and carefully prepared samples. Additionally, a very special thanks to Laura Ponsaerts, Elke Pirlet and Steffie Hasevoets for their help and support with the *in vivo* experiments. I would also like to thank BIOMED for being an excellent institute and for providing the resources for our research. Finally, I appreciate the encouraging environment created by my fellow students, which greatly contributed to this internship.

Author contributions – AB and LA conceived and designed the research. EG performed experiments and data analysis. LA provided assistance with all experiments. EG wrote the paper. All authors carefully edited the manuscript.

SUPPLEMENTAL INFORMATION

Supplemental materials:

dMCAO surgery - Prior to dMCAO surgery, mice were anaesthetised using 3.5% isoflurane (IsoFlo, Abbot Animal Health, Belgium). During surgery, the mice were placed in a lateral position on a warming pad under 2% isoflurane. Additionally, eye ointment (Duratears®, Alcon, Geneva, Switzerland) was applied to prevent drying of the eyes. After shaving and disinfecting the surgical area, a vertical skin incision of ±1-2 cm was made between the ear and eye of the mouse. Reflexes were tested by firmly squeezing the hind legs. The connective tissue surrounding the temporal muscle was removed. The temporal muscle was dissected to expose the skull. A micro drill (Stoelting, Dublin, Ireland) was used to thin out the temporal bone at the site of the bifurcation of the MCA. Using surgical forceps, the skull and meninges overlying the MCA were removed to expose the MCA. Via electrocoagulation, the MCA was permanently occluded by occluding the artery proximally and distally to the bifurcation using bipolar coagulation forceps (0.4mm tip; ERBE, Tuebingen, Germany) with the electrosurgical unit (ERBE ICC 50) set at 8W. The MCA was gently rubbed with two small forceps to ensure permanent occlusion. The wound was sutured with monofilament nylon suture (7-0) and disinfected with Iso-Betadine. After surgery, the mice received 0.05 mg/kg buprenorphine (Temgesic, Val d'Hony Verdifarm, Belgium) subcutaneously for analgesia. For recovery, the mice were placed in a heat recovery cage (32°C) until awakened. Exactly one hour after dMCAO, mice were anaesthetised using 4% isoflurane. The mice were placed in a stereotactic head frame (0.1 µm resolution, Stoelting/David Kopf, Germany) under 2% isoflurane. The skull position was achieved by placing steel rods in the ears of the mice to lift the head. After shaving the head and a 1cm midline incision, the skull was exposed. The treatment was injected into the ventricle according to bregma coordinates (Anterior/posterior: 0; media/lateral: 1mm and dorsal/ventral: -2.2mm). A small hole was drilled according to the predicted injection location. Next, a 10µL Hamilton neuro syringe with needle (VWR, HAMI65460-06) was inserted according to the coordinates, followed by a minute rest. After that, a correction of the dorsal/ventral axis of +0.2mm was made to form the final position for injection. 2µl of treatment was injected at a flow rate of 0.5µL/min. After injection, the needle was left for 2 minutes, after which the syringe was taken out. Histoacryl wound glue (1050052, B. BRAUN, Germany) was used to close the wound. The mice were placed in the heat recovery cage (32°C) until awakened.

Murine NSC isolation – Neural stem cells (NSC) were isolated and cultured according to Gervois *et al. (51).* Shortly, murine NSC were isolated from foetal brains of C57BL/6 mice. At gestational days 14-15, pregnant C57BL/6 mice (Envigo, The Netherlands) were sacrificed by cervical dislocation and the foetuses were removed from the abdomen. The isolated brains were cut into fragments in cold PBS (4°C) containing 100 U/mL penicillin and 100 µg/mL streptomycin (P/S). Following centrifugation (8 min at 200g, MERK), the supernatant was removed and incubated with 0.2% collagenase A (Roche, Basel, Switzerland) and DNase I (2000 Kunitz units/50mL) in PBS for 1.5h at 37°C. The dissociated tissue was washed and resuspended in Neurobasal-A medium supplemented with 1% N2 (Invitrogen), 10 ng/mL epidermal growth factor (EGF) and basic fibroblast growth factor (bFGF) (both from immunotools), 100 U/mL P/S. The NSC cell suspension was rinsed through a 70µm cell strainer and transferred to an uncoated culture flask to allow for neurosphere formation for 4-5 days at 37°C in a humidified atmosphere containing 5% CO_2. Growth factors were replenished every other day. The neurospheres were collected and dissociated with accutase with subsequent seeding at 625,000 cells in a T25 flask with a 5 µg/mL fibronectin (1030-FN-05M, R&D systems, Minneapolis, USA) coated surface.

Scratch-wound-healing assay – A scratch-wound healing assay was performed to investigate the effect of IGFs on direct migration of NSC. NSC cells (passage 24-31) were seeded in an Incucyte ImageLock 96-well plate (Sartorius) with a density of 75,000 cells per well. After 24 hours, when cells reached 100% confluence, standardised wounds were made using the WoundMaker (4563, Sartorius) according to the manufacturer's instructions. Immediately after wounding, the medium was aspirated, and the cells were incubated with test conditions (Table S2). Images were captured every two hours using the IncuCyte® S3 Live-Cell Analysis System for 24 hours. The IncuCyte® Scratch Wound Cell Migration Software Module acquired the wound confluence. The migration assay was independently performed seven times, including four technical replicates.

Supplemental figures and tables:

Table S1: culture media for the different cell types

NSC	NBA medium (10888-022, Gibco, UK) containing 2% B27 minus vitA (12587-010, Gibco), 2mM L-glutamine (G7513, Sigma), 20 ng/mL EGF (11343406, Immunotools, Germany) and bFGF (11343625, Immunotools), and 100 U/mL P/S (P4333, Sigma).
HMEC-1	MCBD 131 medium (10372-019, Gibco) supplemented with 10 mM L-glutamine (G7513, Sigma), 10% Fetal Bovine Serum (FBS) (S181B-500, Biowest, France), 10 ng/mL human EGF (PGH0311L, Gibco), 1 µg/mL hydrocortisone (A16292.03, Alfa Aesar, USA) and 100 U/mL P/S (P4333, Sigma).
Raw264.7	DMEM (41966-052, Gibco) with 10% FBS (S181B-500, Biowest) and 1% P/S (P4333, Sigma).
BMDM	Roswell Park Memorial Institute (RPMI) 1640 medium, GlutoMAX™ supllement (61870036, ThermoFisher), 10% FBS (S181B-500 Biowest), 15% L929 conditioned medium (LCM) and 100 U/mL P/S (P4333, Sigma).

bFGF, basic fibroblast growth factor; BMDM, bone marrow-derived macrophages; DMEM, Dulbecco's Modified Eagle Medium; EGF, epidermal growth factor; FBS, fetal bovin serum; HMEC-1, human microvascular endothelial cells; NBA, neurobasal medium; NSC, neural stem cells, P/S, Penicilline/streptomycine;

Table S2 – Test conditions for *in vitro* and CAM experiments

Assay	Test conditions	Medium
Transwell migration assay	**HCl controls:** 1 and 10 µM	**Transwell medium:** Neurobasal A (NBA) medium (10888-022, Gibco) containing 0.2% B27 minus vitA (12587-010, Gibco), 2mM L-glutamine (G7513, Sigma), 20 ng/mL EGF (11343406, Immunotools) and bFGF (11343625, Immunotools), and 100 U/mL P/S (P4333, Sigma).
	***IGF-II, DES[1-6]IGF-II, Leu^{27}IGF-II :** 100 and 1000 ng/mL	
	***IGF-II or DES[1-6]IGF-II + IGFBP-6:** 100 and 1000 ng/mL + 1000 ng/mL	
	Negative control: transwell medium	
	Positive control: FGF-2 100 ng/mL	
Scratch assay	**HCl controls:** 0.00001, 0.0001, 0.001, 0.01, 0.1, 1 and 10 µM	**Scratch medium:** NBA medium (10888-022, Gibco) containing 0.2% B27 minus vitA (12587-010, Gibco), 2mM L-glutamine (G7513, Sigma), 7.5 ng/mL EGF (11343406, Immunotools) and bFGF (11343625, Immunotools), and 100 U/mL P/S (P4333, Sigma).
	IGF-II: 0.001, 0.01, 0.1 1, 10, 100 and 1000 ng/mL	
	Negative control: scratch medium	
	Positive control: FGF 100 ng/mL	
Proliferation assay	**HCl controls:** 1 and 10 µM	**NSC culture medium:** NBA medium (10888-022, Gibco) containing 2% B27 minus vitA (12587-010, Gibco), 2mM L-glutamine (G7513, Sigma), 20 ng/mL EGF (11343406, Immunotools) and bFGF (11343625, Immunotools), and 100 U/mL P/S (P4333, Sigma).
	IGF-II , DES[1-6]IGF-II, Leu^{27}IGF-II: 100 and 1000 ng/mL	
	Negative control: NSC culture medium	
	Positive control: FGF 100 ng/mL	
Tube formation assay	**HCl controls:** 1 and 10 µM	**Tube formation medium:** Alpha minimum essential medium (A-MEM) (MEMA-XRXA, Capricorn Scientific) supplemented with 2 mM L-Glutamine (G7513, Sigma) and 100 U/mL P/S (P4333, Sigma)
	IGF-II, DES[1-6]IGF-II, Leu^{27}IGF-II: 100 and 1000 ng/mL	
	IGFBP-6: 1000 ng/mL	
	IGF-II or DES[1-6]IGF-II + IGFBP-6: 100 ng/mL + 1000 ng/mL	
	Negative control: Tube formation medium	
	Positive control: 10% FBS A-MEM medium	
ELISA	**IGF-II, DES[1-6]IGF-II:** 100 ng/mL	**Serum-free HMEC-1 medium:** MCBD medium (10372-019, Gibco) containing 0.05% FBS (S181B-500 Biowest), 10 mM L-glutamine (G7513, Sigma) and 100 U/mL P/S (P4333, Sigma)
	IGFBP-6: 1000 ng/mL	
	IGF-II or DES[1-6]IGF-II + IGFBP-6: 100 ng/mL + 1000 ng/mL	
	Negative control: serum-free HMEC-1 medium	
CAM assay	**IGF-II:** 0.5 and 50 **HCl:** 0.5 and 50	0.1%BSA-PBS

* IGF-II (FU100, GroPep, Australia); DES[1-6]IGF-II (MU100, GroPep); Leu^{27}IGF-II (TU100, GroPep); IGFBP-6 (BP6BU100, GroPep)

A-MEM, Alpha minimum essential medium (A-MEM); bFGF, basic fibroblast growth factor; BSA, bovine serum albumin; CAM, Chick chorioallantioc membrane; EGF, epidermal growth factor; ELISA, enzyme-linked immunoassay; FBS, Fetal bovine serum,

HCl, Hydrogencloride; IGF, insulin like growth factor; IGFBP, IGF binding protein; NBA neurobasal medium, P/S, Penicilline/streptomycine;

Table S3: Primary and secondary antibodies used for immunocytochemistry.

Primary Antibody				Secondary Antibody			
Target	Dilution	Reference	Manufacturer	Target	Dilution	Reference	Manufacturer
Goat anti-IGFR1	1:20	NB300-514	Novus Biologicals	Donkey anti-goat Alexa Fluor™555	1:500	A21432	Life Technologies
Mouse anti-IGFR2	1:100	AF-305-NA	R&D systems	Donkey anti-mouse Alexa Fluor™555	1:500	A31570	Life Technologies
Rabbit anti-IR	1:100	NBP2-16970	Novus Biologicals	Goat anti-rabbit Alexa Fluor™555	1:500	A21430	Life Technologies

IGFR1, insulin-like growth factor receptor type 1; IGFR2, insulin-like growth factor receptor type 2; IR, insulin receptor

Table S4: Primary and secondary antibodies used for immunofluorescence.

Primary Antibody				Secondary Antibody			
Target	Dilution	Reference	Manufacturer	Target	Dilution	Reference	Manufacturer
Goat anti-IGFR1	1:20	NB300-514	Novus Biologicals	Donkey anti-goat Alexa Fluor™555	1:500	A21432	Life Technologies
Mouse anti-IGFR2	1:100	AF-305-NA	R&D systems	Donkey anti-mouse Alexa Fluor™555	1:500	A31570	Life Technologies
Rabbit anti-IR	1:100	NBP2-16970	Novus Biologicals	Goat anti-rabbit Alexa Fluor™555	1:500	A21430	Life Technologies
Rabbit anti-Iba1	1:250	N019-19741	Wako Pure Chemical	Goat anti-rabbit Alexa Fluor™500	1:500	A21430	Life Technologies
Rabbit anti-NF	1:200	171 002	Synaptic Systems	Goat anti-rabbit Alexa Fluor™500	1:500	A21430	Life Technologies

Iba1, ionised calcium-binding adaptor molecule 1; IGFR1, insulin-like growth factor receptor type 1; IGFR2, insulin-like growth factor receptor type 2; IR, insulin receptor; NF, neurofilament.

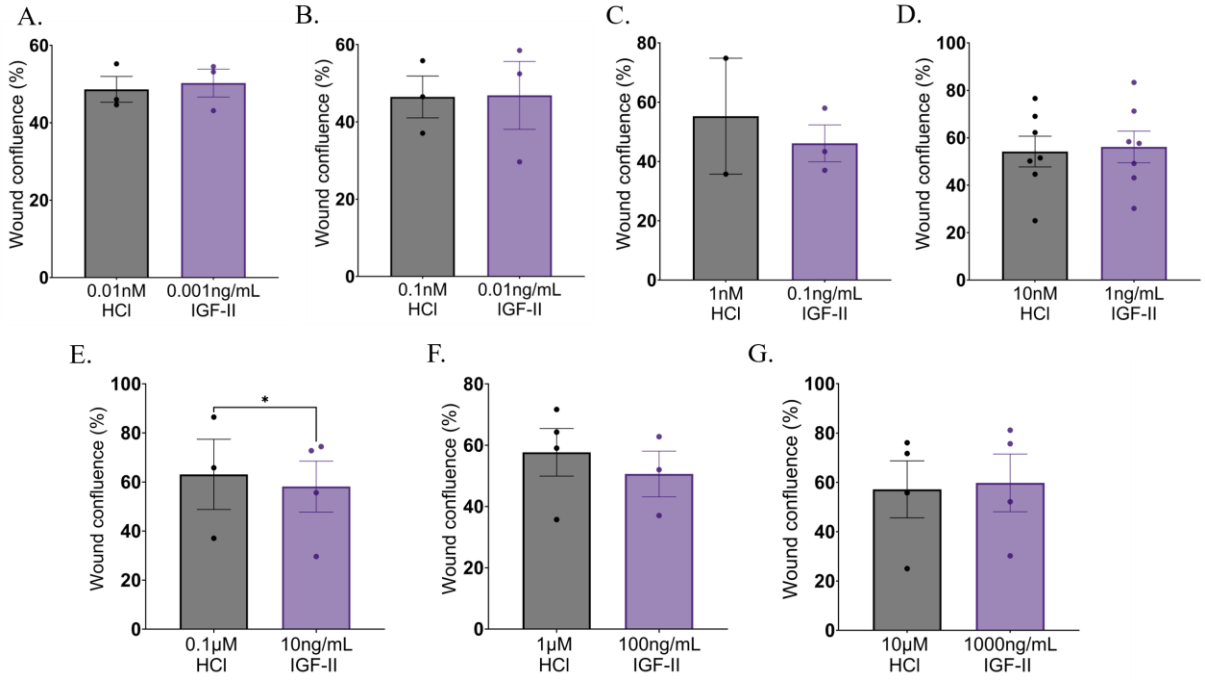

Figure S1: IGF-II Does Not Stimulate Direct NSC Migration. The effects of IGF-II on NSC migration were assessed using a scratch-wound-healing assay. **A-G.**The graphs illustrate the wound confluence of various concentrations of IGF-II and their corresponding HCl control 8 hours after the initial wound making. Not a single concentration of IGF-II significantly stimulated NSC migration compared to their HCl control. **E.** Compared to HCl control, IGF-II at 10 ng/mL significantly reduced the NSC migration. **A-G.** Data are expressed as mean ± SEM. N = 2-7 with 2-4 replicates per condition. Each data point represents an independent assay. *p<0.05. Statistical analysis was performed using a paired t-test. *HCl, hydrochloric acid; IGF, insulin-like growth factor; NSC, neural stem cells; SEM, standard error of the mean.*

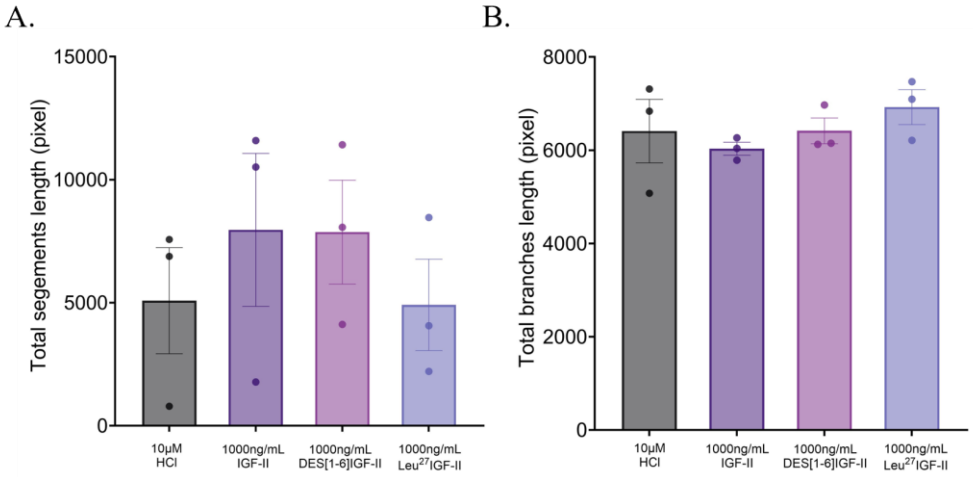

Figure S2 – **IGF-II Does Not Stimulate Tube Formation at 1000 ng/mL. A.** The effect of IGF variants on the total segment length in the tube formation assay after 6 hours. While neither IGF variant significantly stimulated segments, a positive trend is visible. **B.** The effect of IGF variants on total branch length in the tube formation assay after 6 hours. Again, neither IGF variant significantly stimulated branch formation. **A and B.** Data are expressed as mean ± SEM. N = 3 with 2-3 replicates per condition. Each data point represents an independent assay. Statistical analysis was performed using RM one-way ANOVA with Dunnett's post hoc test. *HCl, hydrochloric acid; IGF, insulin-like growth factor; RM, repeated measures; SEM, standard error of the mean.*

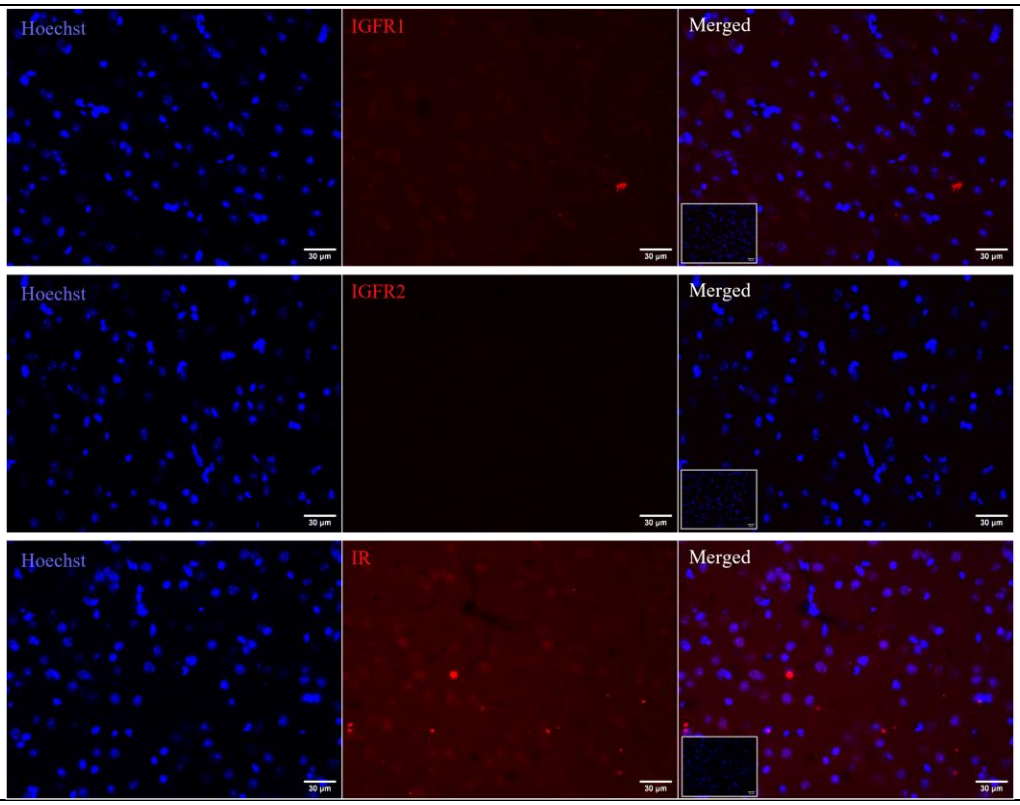

Figure S3 – **The presence of IGF-II receptors on healthy murine brain coupes.** Representative images of immunofluorescent staining show the presence of the three IGF-II receptors (red) – IGFR1 (top panel), IGFR2 (middle panel), and IR (bottom panel) – on healthy murine brain coupes. The IR (bottom panel) and, to a lesser extent, the IGFR1 (top panel) are present in the healthy brain, while IGFR2 (middle panel) does not indicate presence. Nuclei were counterstained with Hoechst (blue). Insert shows the negative control. Scale bar represents 30µm. *IGFR1, insulin-like growth factor receptor type 1; IGFR2, insulin-like growth factor receptor type 2; IR, insulin receptor*

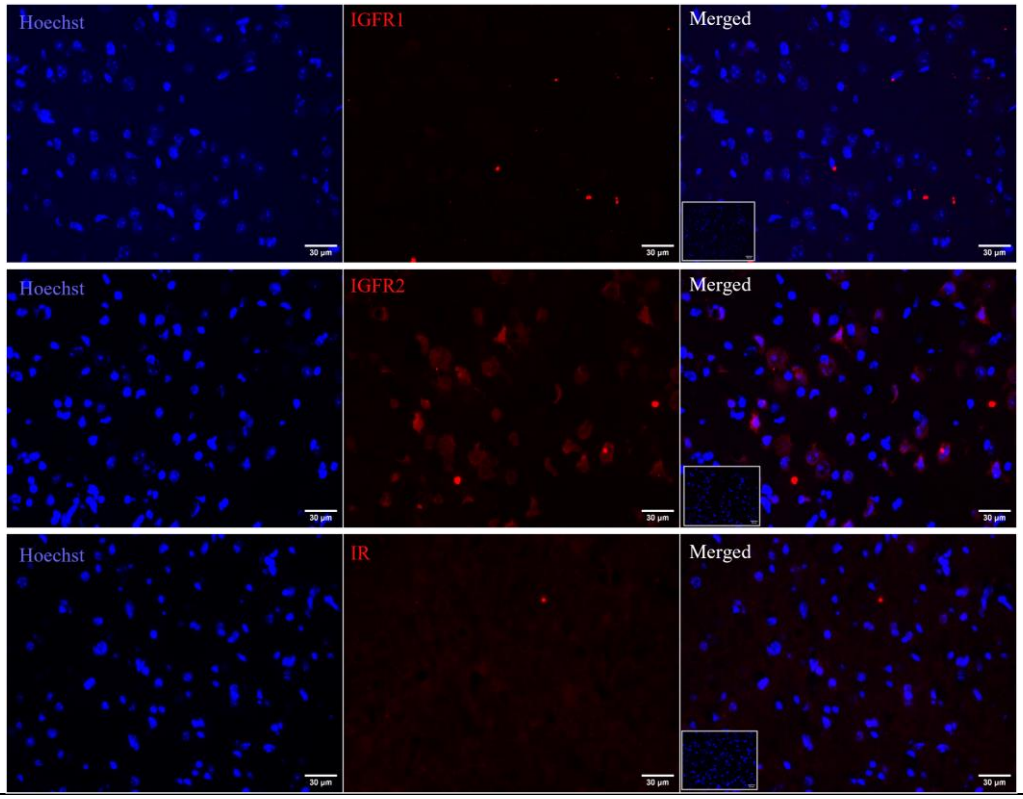

Figure S4 – **The presence of IGF-II receptors on murine dMCAO brain coupes three days post-stroke.** Representative images of immunofluorescent staining show the presence of the three IGF-II receptors (red) – IGFR1 (top panel), IGFR2 (middle panel), and IR (bottom panel) – on murine dMCAO brain coupes three days post-stroke. The IR (bottom panel) and the IGFR1 (top panel) indicate very little to no presence, while IGFR2 (middle panel) is present. Nuclei were counterstained with Hoechst (blue). Insert shows the negative control. Scale bar represents 30µm. *dMCAO, distal middle cerebral artery occlusion model; IGFR1, insulin-like growth factor receptor type 1; IGFR2, insulin-like growth factor receptor type 2; IR, insulin receptor*

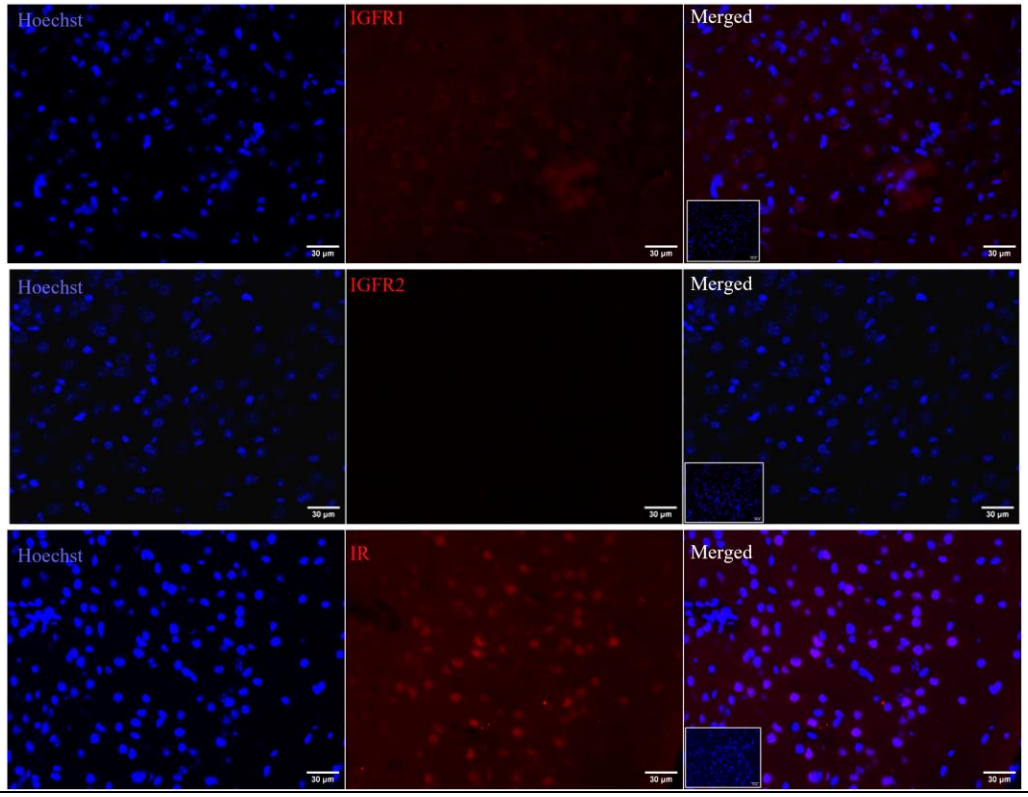

Figure S5 – **The presence of IGF-II receptors on murine dMCAO brain coupes seven days post-stroke.** Representative images of immunofluorescent staining show the presence of the three IGF-II receptors (red) – IGFR1 (top panel), IGFR2 (middle panel), and IR (bottom panel) – on murine dMCAO brain coupes seven days post-stroke. The IR (bottom panel) and, to a lesser extent, the IGFR1 (top panel) are present in the murine dMCAO brain seven days post-stroke, while IGFR2 (middle panel) does not indicate presence. Nuclei were counterstained with Hoechst (blue). Insert shows the negative control. Scale bar represents 30µm. *dMCAO, distal middle cerebral artery occlusion model; IGFR1, insulin-like growth factor receptor type 1; IGFR2, insulin-like growth factor receptor type 2; IR, insulin receptor*

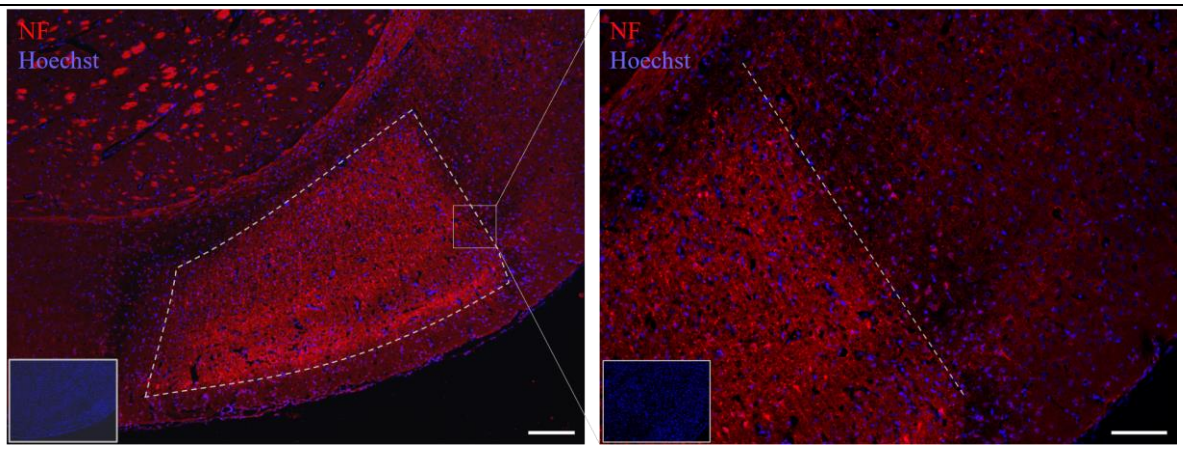

Figure S6 – **The identification of a suitable ischemic stroke lesion marker.** Representative images of immunofluorescent staining of a murine dMCAO brain coupe seven days post-stroke show the neurofilament 68 kD (NF) marker (red), which outlines the stroke area by increased immunoreactivity (left panel – white dashed area). Scale bar represents 200 µm. The border of the stroke area is distinguishable from the healthy tissue due to the increased immunoreactivity (right panel – white dashed line). Scale bar represents 120 µm. Nuclei were counterstained with Hoechst (blue). Insert shows the negative control. *dMCAO, distal middle cerebral artery occlusion model; NF, neurofilament*